WOODHEAD PUBLISHING SERIES IN COMPOSITES SCIENCE AND ENGINEERING

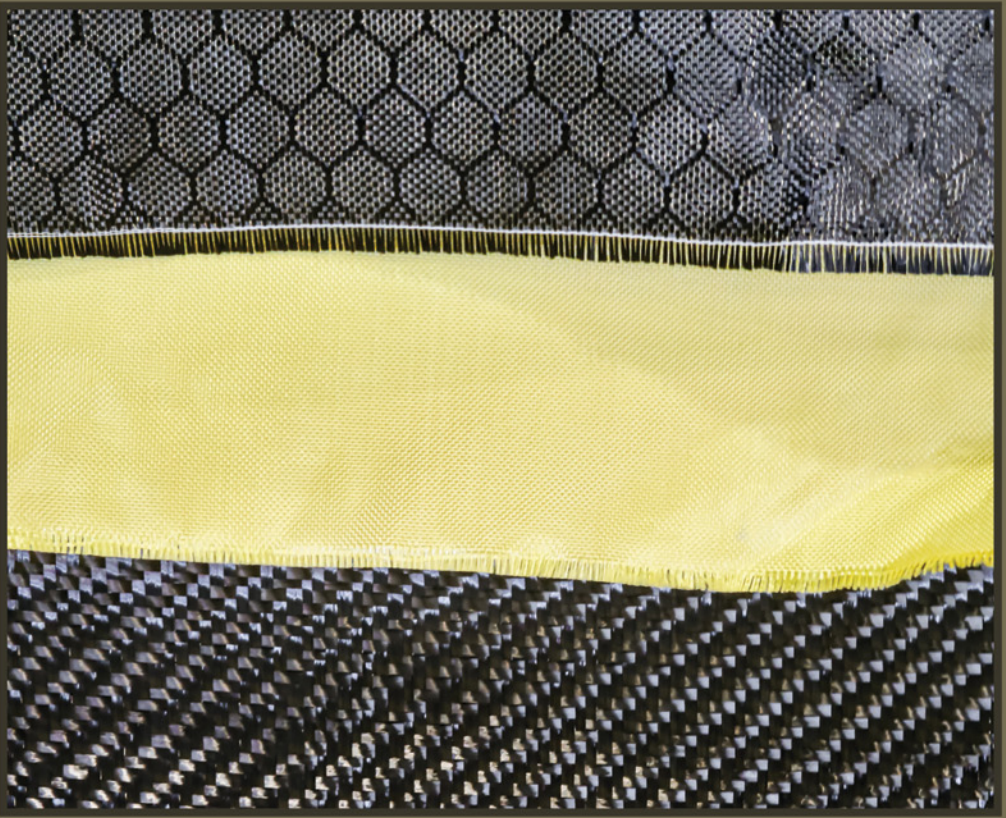

SMART BIOCOMPOSITE MATERIALS

FABRICATION, APPLICATIONS, AND SUSTAINABILITY

Edited by
MD. REZAUR RAHMAN
MUHAMMAD KHUSAIRY BIN BAKRI

ELSEVIER

Smart Biocomposite Materials

The **Woodhead Publishing Series in Composites Science and Engineering** is a suite of professional reference books providing comprehensive coverage of recent developments in composite materials research for application now and in the future.

Woodhead Publishing Series in Composites Science and Engineering

Smart Biocomposite Materials

Fabrication, Applications, and Sustainability

Edited by

Md. Rezaur Rahman

Muhammad Khusairy Bin Bakri

WP
WOODHEAD PUBLISHING
An imprint of Elsevier

Woodhead Publishing is an imprint of Elsevier
50 Hampshire Street, 5th Floor, Cambridge, MA 02139, United States
125 London Wall, London EC2Y 5AS, United Kingdom

Notices

Knowledge and best practice in this field are constantly changing. As new research and experience broaden our understanding, changes in research methods, professional practices, or medical treatment may become necessary.

Practitioners and researchers must always rely on their own experience and knowledge in evaluating and using any information, methods, compounds, or experiments described herein. In using such information or methods they should be mindful of their own safety and the safety of others, including parties for whom they have a professional responsibility.

To the fullest extent of the law, neither the Publisher nor the authors, contributors, or editors, assume any liability for any injury and/or damage to persons or property as a matter of products liability, negligence or otherwise, or from any use or operation of any methods, products, instructions, or ideas contained in the material herein.

ISBN: 978-0-443-33643-0 (print)
ISBN: 978-0-443-33644-7 (online)

For information on all Woodhead Publishing publications
visit our website at https://www.elsevier.com/books-and-journals

Publisher: Matthew Deans
Acquisitions Editor: Gwen Jones
Editorial Project Manager: Sonal Nagpal
Production Project Manager: Maria Bernard
Cover Designer: Gopalakrishnan Venkatraman

Typeset by MPS Limited, Chennai, India

Dedication

This work is dedicated to my amazing wife and daughters, Shirin Akther, Fahriah Rahman, and Faizah Rahman, who are very special to me and made it possible for me to complete this work.

—Associate Professor Ts. Dr. Md. Rezaur Rahman

First, I would like to thank the Almighty God for the guidance, strength, power of mind, protection, and for giving us a healthy life. All of these we offer to you. Every difficult task needs self-effort as well as the guidance of elders, particularly those who are near to our hearts. I offer my humble dedications to my beautiful and loving father, mother, wife, and brothers, whose devotion, love, support, and nightly prayers have enabled me to work toward this significant achievement, along with all the dedicated, well-liked, and well-respected teachers and supervisors.

—Ts. Dr. Hj. Muhammad Khusairy Bin Bakri

This page intentionally left blank

Contents

List of contributors

M. Kaisher Ahmed Department of Chemistry, University of Chittagong, Chittagong, Bangladesh

Muhammad Khusairy Bin Bakri Faculty of Engineering, Universiti Malaysia Sarawak, Kota Samarahan, Sarawak, Malaysia; Composite Materials and Engineering Center, Washington State University, Pullman, WA, United States

Chiu Po Chan Faculty of Computer Science and Information Technology, Universiti Malaysia Sarawak, Kota Samarahan, Sarawak, Malaysia

Faisal Islam Chowdhury Department of Chemistry, University of Chittagong, Chittagong, Bangladesh

Sinin Hamdan Department of Mechanical and Manufacturing Engineering, Faculty of Engineering, Universiti Malaysia, Kota Samarahan, Sarawak, Malaysia

M. Rahnuma Iqbal Ifte Department of Chemistry, University of Chittagong, Chittagong, Bangladesh

Anthonette Anak James Department of Chemical Engineering and Energy Sustainability, Faculty of Engineering, University of Malaysia, Kota Samarahan, Sarawak, Malaysia

Anjelina Joffery Kalimuthu Faculty of Engineering, Universiti Malaysia Sarawak, Kota Samarahan, Sarawak, Malaysia

Perry Law Nyuk Khui Faculty of Engineering, Universiti Malaysia Sarawak, Kota Samarahan, Sarawak, Malaysia

Kuok King Kuok Faculty of Engineering, Computing and Science, Swinburne University of Technology, Sarawak Campus, Kuching, Sarawak, Malaysia

Mohammad Abdul Mannan Faculty of Engineering, Universiti Malaysia Sarawak, Kota Samarahan, Sarawak, Malaysia

Lelly Marini Faculty of Engineering, Universiti Malaysia Sarawak, Kota Samarahan, Sarawak, Malaysia

Ain Nadirah Binti Mohd Sufian Faculty of Engineering, Universiti Malaysia Sarawak, Kota Samarahan, Sarawak, Malaysia

Murtala Namakka Faculty of Engineering, Universiti Malaysia Sarawak, Kota Samarahan, Sarawak, Malaysia

Md. Rezaur Rahman Faculty of Engineering, Universiti Malaysia Sarawak, Sarawak, Kota Samarahan, Malaysia

Khairul Anwar Mohamad Said Faculty of Engineering, Universiti Malaysia Sarawak, Kota Samarahan, Sarawak, Malaysia; Department of Chemical Engineering and Energy Sustainability, Faculty of Engineering, UNIMAS Water Centre (UWC), Universiti Malaysia, Kota Samarahan, Sarawak, Malaysia; UNIMAS Water Centre, Faculty of Engineering, Universiti Malaysia, Kota Samarahan, Sarawak, Malaysia

Ain Zaienah Sueraya Department of Chemical Engineering and Energy Sustainability, Faculty of Engineering, University of Malaysia, Kota Samarahan, Sarawak, Malaysia

Nur-Azzah Afifah binti Taib Faculty of Engineering, University Malaysia Sarawak, Kota Samarahan, Sarawak, Malaysia

About the editors

Ts. Dr. Md. Rezaur Rahman is an Associate Professor in the Department of Chemical Engineering and Energy Sustainability, Faculty of Engineering, Universiti Malaysia Sarawak (UNIMAS), Malaysia. Since 2012 he has also served as a Visiting Research Fellow at the Faculty of Engineering, Tokushima University, Japan. His academic journey includes experience as a Teaching Assistant at Bangladesh University of Engineering and Technology (BUET) and as a Research Project Leader under the Malaysian Ministry of Higher Education. In 2015 he was appointed as an External Supervisor at the Faculty of Engineering, Swinburne University of Technology, Melbourne, Australia. Dr. Rahman holds a PhD from UNIMAS and brings over 12 years of experience in teaching, research, and industry collaboration. His research expertise spans conducting polymers, nanocomposites, and advanced materials, including graphene, nanoclay, fire retardants, and nanocellulose-reinforced polymer composites. He has made significant contributions to the development of hybrid-filled polymer blends and the chemical modification of lignocellulosic fibers, such as jute, coir, and kenaf. To date, Dr. Rahman has authored 7 books, 20 book chapters, and over 200 articles in international journals, establishing himself as a prominent researcher in polymer science and nanotechnology. He is also listed in Stanford University's Top 2% Scientists list of the world's most cited scientists.

Ts. Dr. Hj. Muhammad Khusairy Bin Capt. Hj. Bakri is a Postdoctoral Research Associate at Washington State University (WSU), specializing in materials and mechanical engineering. He holds a PhD (2018), MEng (2016), and BEng (2014) from Swinburne University of Technology. Dr. Khusairy's research focuses on enhancing the durability, interfacial interaction, and stability of composites through advanced thermal and chemical treatments, with an emphasis on biocomposites for sustainable and economically viable applications. With expertise in wood composites, biocomposites, biomaterials, and wastewater treatment, he has published over 279 scholarly works, including journal articles, book chapters, newspaper/bulletin, and conference proceedings. Dr. Khusairy has previously served as a Research Fellow at UNIMAS and has collaborated on international research projects across Malaysia and abroad. A certified Graduate Engineer and Professional Technologist under the Malaysian Board of Technologists (MBOT), he is also a lifetime member of the Association of Professional Technicians and Technologists (APTT). Dr. Khusairy's contributions have been recognized internationally, including being a finalist for the Alumni Impact Awards 2022 and featured in Successful People in Malaysia, 2023.

This page intentionally left blank

Preface

Materials science has now reached a critical phase of development, where combining sustainability, intelligence, and functionality is no longer visionary but the absolute requirement of the time. While the world is facing increasingly aggravated environmental concerns and its industries face growing demands for responsive and high-performance materials, the combination of biobased components with intelligent attributes is an opportunity for innovation, at the same time as it is eco-friendly and technologically advanced.

Intelligent biocomposite materials are one class of engineered systems combining renewable natural fibers with biodegradable or recyclable matrices and functional fillers or additives with responsive behaviors to external stimuli. These materials successfully address the imperative of reducing dependency on fossil-derived resources and possess enhanced features like self-healing, shape memory, and active sensing or actuation functions as well. The last 10 years have seen tremendous development in this field, driven by interdisciplinarity among materials engineering, biotechnology, polymer science, nanotechnology, and applied mechanics.

At the core of this discussion is a deep understanding of the interactions between different components, natural fibers, polymer matrices, and added functionalities. Advances in fabrication technologies, ranging from conventional compounding methods to advanced additive manufacturing methods, have enabled the large-scale production of biocomposites with tailored mechanical, thermal, and functional properties. The combination of responsive functionalities, such as sensors, stimuli-responsive fillers, or drug delivery systems, greatly expands their utility in high-end markets, such as biomedical devices, aerospace components, structural health monitoring, and soft robotics.

An important aspect of research in this area is mirroring the built-in self-sufficiency of nature with the development of materials with self-healing tendencies, the ability to change their shape in the presence of outside stimuli, and the ability to perform regulated-release functions. These attributes improve the potential of biocomposites and open up new prospects for research and application.

Sustainability remains the underlying tenet of this field, including not just the origin of materials but also life cycle assessment, recyclability, and environmental impact considerations. As the world economy increasingly moves toward more circular and biobased models of development, novel biocomposites are expected to play a key role in enabling this transformational process.

This book aims to act as a comprehensive scholarly reference for researchers, engineers, and postgraduate instructors to explore the scientific basis, processing methodologies, functional characteristics, and potential uses of intelligent

biocomposite materials. This book integrates fundamental knowledge and state-of-the-art advancements to prompt further research and enable the development of advanced materials with features like intelligence, long-term performance, and sustainability.

Associate Professor Ts. Dr. Md. Rezaur Rahman
Ts. Dr. Hj. Muhammad Khusairy Bin Capt. Hj. Bakri

Challenges and future directions of biocomposite materials

14

Lelly Marini[1], *Mohammad Abdul Mannan*[1], *Md. Rezaur Rahman*[1], *and Muhammad Khusairy Bin Bakri*[1,2]
[1]Faculty of Engineering, Universiti Malaysia Sarawak, Kota Samarahan, Sarawak, Malaysia, [2]Composite Materials Engineering Center, Washington State University, Pullman, WA, United States

14.1 Introduction

Biocomposite materials, comprising natural fibers and bio-based or synthetic matrices, have emerged as promising solutions in the pursuit of sustainable alternatives to conventional materials. Their rise in prominence is fueled by growing environmental awareness and the implementation of stringent regulations aimed at curbing greenhouse gas emissions. The global biocomposites market, valued at $24.4 billion in 2020, is projected to reach $51.2 billion by 2027, reflecting a robust compound annual growth rate of 11.3% (Gomes et al., 2019). This growth underscores the increasing adoption of biocomposites across diverse industries.

In the construction sector, biocomposites find applications in insulation panels, roofing sheets, and modular components, offering lightweight and eco-friendly alternatives to traditional materials. The automotive industry integrates biocomposites into lightweight interior parts, enhancing fuel efficiency and reducing vehicle emissions. Meanwhile, the packaging industry benefits from biodegradable containers and films, which address the dual challenges of plastic waste and reliance on fossil-based resources. These applications collectively contribute to reduced carbon footprints and the advancement of circular economy principles.

The development of biocomposites shares parallels with innovations in geopolymer concrete, another sustainable material designed to mitigate environmental impact. Geopolymer concrete achieves significant reductions in CO_2 emissions—up to 80% compared to conventional Portland cement—by utilizing industrial by-products such as fly ash (FA) and slag (Institutes, n.d.). Similarly, biocomposites incorporate agricultural residues and natural fibers, transforming waste into valuable resources while promoting sustainability and resource efficiency.

Despite these advancements, biocomposites face critical challenges, including variability in raw material properties, limited mechanical strength compared to synthetic composites, and scalability issues in production processes. Overcoming these barriers demands a multidisciplinary approach, integrating expertise from material science, engineering, and industry collaborations (Adamu et al., 2019; Amran et al., 2021; Bakri et al., 2018; Fatema et al., 2024; Hari et al., 2021; James et al., 2024; Jayamani et al., 2015, 2016; Jayamaui et al., 2020). Drawing lessons

Smart Biocomposite Materials. DOI: https://doi.org/10.1016/B978-0-443-33643-0.00011-9

from the success of geopolymer concrete, tailored strategies can be developed to advance biocomposite technologies, aligning them with global sustainability objectives (Sax, 2024).

This chapter delves into the challenges and opportunities associated with biocomposite materials, offering insights into innovative solutions and future directions. By leveraging the lessons learned from sustainable materials like geopolymer concrete, the discussion aims to chart a comprehensive roadmap for the evolution of biocomposites, ensuring their role as key enablers of a sustainable future.

14.2 Challenges in biocomposite material development

14.2.1 Raw material availability and variability

Biocomposites rely heavily on agricultural and forestry by-products, such as hemp, flax, jute fibers, and other natural sources. The availability of these raw materials is subject to seasonal variations, geographical differences, and agricultural practices, making supply chains unpredictable. For example, hemp production is influenced by soil quality and climate, while flax yields can vary due to pest infestations and harvesting techniques. Furthermore, natural fibers exhibit significant variability in mechanical properties such as tensile strength, elasticity, and moisture content (Delgado-Plana et al., 2021; Kanagaraj, Lubloy, et al., 2023; Kiew et al., 2013; Kuok et al., 2024; Lai et al., 2015; Namakka, Rahman, Bin Mohamad Said, et al., 2024; Namakka, Rahman, Mohamad Bin Said, et al., 2024). This variability complicates efforts to ensure consistent composite performance, requiring advanced sorting, grading, and pretreatment methods to homogenize raw materials. Addressing these issues necessitates investment in cultivation technologies, such as genetically optimized crops, and the development of regional supply chains to stabilize raw material access.

14.2.2 Balancing mechanical performance with sustainability

While biocomposites are celebrated for their eco-friendliness, their mechanical properties often fall short compared to synthetic composites. For instance, natural fibers like jute and hemp have lower tensile strengths than glass or carbon fibers, which limits their use in high-performance applications. Poor fiber-matrix adhesion is another critical issue, as weak bonding reduces load transfer efficiency, leading to premature failure under stress. Moisture sensitivity exacerbates these problems, as natural fibers tend to swell and degrade in humid environments. Strategies to address these challenges include the use of coupling agents, such as silanes, to improve adhesion, and chemical or thermal treatments to reduce moisture absorption. Additionally, hybrid composites that combine natural and synthetic fibers are being explored to enhance mechanical performance while retaining sustainability benefits.

14.2.3 Cost and scalability

High production costs and limited scalability remain significant barriers to the commercial viability of biocomposites. The pretreatment and processing of natural

fibers to meet industrial standards often require specialized equipment and energy-intensive methods, increasing production expenses. For instance, alkali treatments to improve fiber compatibility with matrices can be costly and time-consuming. The development of bio-based matrices, such as polylactic acid, further adds to the cost due to their complex synthesis processes. Additionally, inconsistent raw material supply disrupts large-scale production, driving up costs through inventory adjustments and procurement challenges. To overcome these barriers, cost-effective processing methods, such as enzymatic treatments, and the establishment of industrial-scale production facilities are critical. Government subsidies and incentives for sustainable materials can also play a key role in addressing cost concerns.

14.2.4 Processing and standardization

The lack of standardized processing techniques and quality control methods is a major obstacle to the widespread adoption of biocomposites. Natural fibers require extensive pretreatment to remove impurities, enhance mechanical properties, and improve compatibility with polymer matrices. However, these processes often vary between manufacturers, leading to inconsistent product quality. Furthermore, the absence of universally accepted standards for testing and certifying biocomposites makes it difficult for industries to adopt them with confidence. For example, the tensile strength of biocomposites can vary significantly depending on the testing methods used, creating uncertainty in performance metrics. Initiatives to establish global standards for biocomposite processing and certification, similar to ASTM standards for conventional materials, are essential for industry growth.

14.2.5 Durability and life cycle assessment

Biocomposites are prone to degradation under environmental conditions such as high humidity, UV exposure, and microbial activity. For example, jute fibers can lose up to 50% of their tensile strength after prolonged exposure to moisture, limiting their use in outdoor applications. UV radiation can also cause discoloration and embrittlement of natural fibers, further compromising performance. Comprehensive life cycle assessments (LCAs) are needed to validate the environmental benefits of biocomposites across their production, use, and disposal phases. Such assessments must consider factors like energy consumption during processing, transportation emissions, and end-of-life disposal options. Innovations such as UV-resistant coatings, biodegradable resins, and recycling technologies can enhance the durability and sustainability of biocomposites, making them more competitive with synthetic alternatives.

14.3 Case study insights: lessons from geopolymer concrete

The optimization strategies employed in geopolymer concrete—a sustainable alternative to conventional concrete—offer valuable insights for biocomposite development. Geopolymer concrete's emphasis on silica-alumina ratio optimization

to enhance mechanical properties parallels the need for precise fiber-matrix compatibility in biocomposites. Concrete is the most widely used construction material globally (Vázquez-Calle et al., 2022), but traditional Portland cement, its main binder, is a significant source of CO_2 emissions (Marini et al., 2024), contributing to climate change (Neupane, 2022). To address this, geopolymer concrete has emerged as a more sustainable alternative (Ndagi & Saleh Jaafar, 2019). By replacing Portland cement with industrial by-products (Kathirvel & Sreekumaran, 2021), geopolymer concrete reduces carbon emissions while repurposing waste (Wong, 2022). It also offers excellent mechanical properties for high-performance applications (Qaidi, Sulaiman Atrushi, et al., 2022). Haruna et al. (2020) noted that adding slag can extend setting time and enhance strength. This research explores using FA, slag, silica fume, and steel fibers (STF) in the geopolymer matrix to produce ultrahigh-strength concrete. Slag, rich in silica and alumina, promotes geopolymerization (Pacheco-Torgal et al., 2013), forming a dense microstructure primarily composed of C–A–S–H gel, which improves compressive strength (Castillo et al., 2021). The key reaction involves dissolving silica and alumina (Chuah et al., 2016) from source materials using an alkaline activator (Madirisha et al., 2024), forming a rigid three-dimensional Si–O–Al network (Chuewangkam et al., 2024) that gives the material its strength (Kushwah et al., 2021). The Si/Al ratio is crucial in controlling the composition and density of the matrix (Chiranjeevi et al., 2023; Siddika et al., 2021), with a higher ratio increasing compressive strength by producing a more silica-rich structure. N–A–S–H gel, the main binding phase, is also influenced by the Si/Al ratio (Chen et al., 2024), which affects both mechanical properties and chemical stability (Li et al., 2020).

Fig. 14.1 shows in Portland cement concrete derives its strength from hydration reactions that form calcium–silicate–hydrate (C–S–H) gel, creating a robust internal

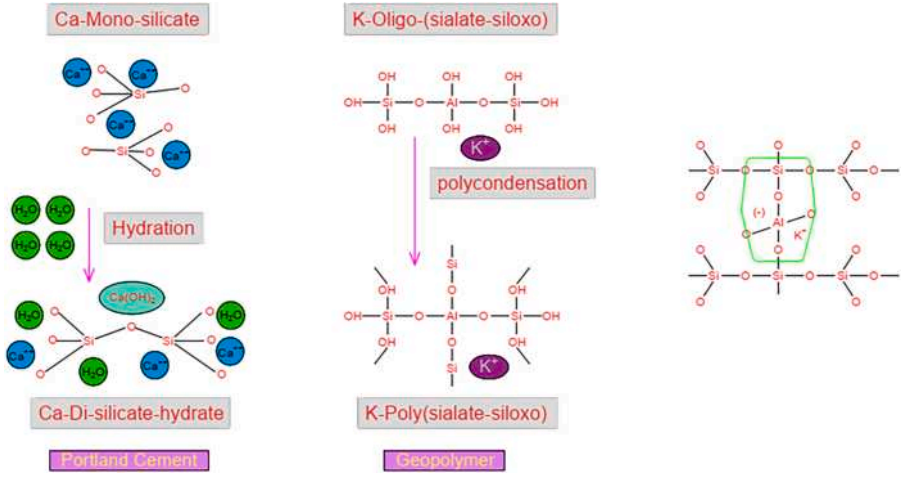

Figure 14.1 The comparison of polymer bonding that occurs between Portland cement concrete and geopolymer concrete.

structure (Madadi & Wei, 2022). In contrast, geopolymer concrete uses polymerization of aluminosilicate materials activated by alkaline solutions, resulting in a unique Si–O–Al bonding network (Cui et al., 2023). This difference influences the mechanical properties and performance of each concrete type. Researchers assess these mechanisms to identify which offers better structural integrity and environmental sustainability. STF enhance tensile strength, ductility, and crack resistance by bridging microcracks (Alashker & Raza, 2022; Liu et al., 2020; Zheng et al., 2023). The combination of dense C–A–S–H gel and STF allows geopolymer concrete to achieve strength comparable to high-performance concretes. However, higher costs associated with alkali activators like sodium silicate pose challenges (Rintala et al., 2021; Tempest et al., 2015), making it essential to optimize the Si/Al ratio for better mechanical properties and economic viability.

Research shows a strong correlation between the Si/Al ratio and the mechanical properties of geopolymer concrete. Higher Si/Al ratios enhance compressive, tensile, and flexural strength by creating a denser matrix (Alaneme et al., 2024; Tu & Zhang, 2023). SiO_2 increases silicate chain rigidity, while Al_2O_3 improves cross-linking (Hajiabadi et al., 2023). For ultrahigh-strength applications, optimizing the Si/Al ratio is crucial for achieving compressive strengths over 100 MPa (Castillo et al., 2021). Alkali-activated waste materials, such as FA and NaOH, initiate aluminosilicate reactions that strengthen the matrix (Almutairi et al., 2021). The combination of Na_2SiO_3 and NaOH or other alkali activators like KOH is especially effective at higher Si/Al ratios (Lăzărescu et al., 2017). Liu et al. (2020) achieved 170.4 MPa with a 5.1 Si/Al ratio, while Althoey et al. (2023) reached 155.4 MPa at 8.95. Higher NaOH molarities improve strength (Ahmad Sofri et al., 2020), but lower Si/Al ratios can limit compressive strength to below 80 MPa (Kucukgoncu & Özbayrak, 2024). Curing conditions also play a vital role. Oven curing at 60°C–90°C for 24–72 hours significantly boosts strength, with Lao et al. (2022), Lao et al. (2023) achieving 222 MPa at 90°C for 72 hours. Tahwia et al. (2022) reached 152MPa with a higher Si/Al ratio of 8.73. In contrast, lower ratios (1.5–3.0) generally result in compressive strengths below 80 MPa, as shown by Palomo et al. (1999) and Abdullah et al. (2017). Ambient curing results in much lower strengths (Palomo et al., 1999). Compressive strengths range from 13 MPa with ferronickel slag to 222 MPa with a mix of FA, ground granulated blast-furnace slag (GGBS), and SF (Althoey et al., 2023; Gao et al., 2024). The use of these materials, especially at higher Si/Al ratios, is effective in producing high-performance geopolymer concrete. Flexural strength varied as well, with Gao et al. (2024) reaching 21.11 MPa using kaolin and silica powder, while Lao et al. (2022) obtained 18 MPa with a similar FA, GGBS, and SF mix. The inclusion of waste materials and additives like GGBS and SF significantly enhances compressive strength, especially with higher Si/Al ratios. Liu et al. (2020) reached 170.3 MPa using GGBS and FA, while Tahwia et al. (2022) and Althoey et al. (2023) achieved strengths over 150 MPa with high Si/Al ratios and additives. This highlights the effectiveness of these materials and ratios in producing high-performance geopolymer concrete.

Balancing strength and weight reduction is essential for lightweight concrete (Bhaidas et al., 2024), which uses lower specific gravity materials to decrease density while maintaining strength (Rodacka et al., 2023). Incorporating waste materials can

enhance mechanical properties (Singh & Kumar, 2024) but may lead to lower overall strength and increased brittleness compared to normal-weight concrete (Bakhoum & Mater, 2022; Hong et al., 2022; Rumsys et al., 2018). Lightweight geopolymer concrete offers reduced structural weight without sacrificing strength (Kanagaraj, Anand, et al., 2023). Achieving ultra-high-strength alongside lightweight properties requires careful design (Iffat, 2016; Wang et al., 2024). High-reactivity materials like FA, GGBS, and SF improve microstructure without significantly increasing density, while strong alkali activators and optimal curing conditions enhance strength. Incorporating STF can also boost flexural and tensile strength without adding weight (Ma et al., 2023). Optimizing the Si/Al ratio within 4.0–8.95 is crucial for maximizing both compressive and flexural strength, facilitating a balance between high performance and reduced weight. This study aims to identify the optimal Si/Al ratio through predictive modeling and experimental validation, contributing to sustainable, high-strength concrete solutions. Kalinowska-Wichrowska et al. (2022), Kalinowska-Wichrowska et al. (2022) found that using FA and GGBS in lightweight geopolymer concrete significantly enhances compressive strength and reduces water absorption. The optimal mix included 400 kg/m³ of additives and 10 M NaOH, with presoaked lightweight aggregates improving adhesion and microstructure density (Rahardjo et al., 2024). High-density lightweight concrete (1350–1850 kg/m³) (Zaki et al., 2021) reduces reinforcement needs and enhances thermal and flexural performance. Other studies reported densities of 1850–1951 g/cm³ with compressive strengths of 24.5–50.3 MPa (Abbas et al., 2018; Nukah et al., 2024; Rajalekshmi & Jose, 2023). This research aims to optimize the Si/Al ratio and increase SiO_2 and Al_2O_3 content to achieve ultra-high-strength while maintaining reduced weight. Mechanical tests and microstructural analyses [scanning electron microscopy (SEM)–energy dispersive spectroscopy (EDS), FTIR] will evaluate the effects of these ratios and STF, with advanced models (ANN, XGB, MLR) optimizing mix design and validating predictions through experiments.

14.3.1 Material optimization

Geopolymer concrete demonstrates the importance of fine-tuning material ratios and curing conditions to maximize performance. For example, optimizing the silica–alumina ratio in geopolymer concrete has resulted in compressive strengths exceeding 100 MPa, highlighting the critical role of composition in achieving high performance. Similarly, biocomposites can benefit from advanced modeling techniques to optimize fiber volume fractions, matrix formulations, and processing conditions (Namakka et al., 2023; Qaidi, Najm, et al., 2022; Rahman et al., 2011, 2013, 2017, 2019, 2024; Rahman, Hamdan, Hasan, et al., 2015; Rahman, Hamdan, Hashim, et al., 2015; Sueraya et al., 2024). Adjusting the proportion of natural fibers and resin, for instance, can significantly influence tensile strength and impact resistance. Curing conditions, such as temperature and humidity, also play a key role in ensuring optimal bonding and structural integrity in biocomposites.

This study employed several key materials in the production of geopolymer concrete, all of which are classified as scheduled waste and are abundantly available

in Sarawak, Malaysia. These materials include industrial by-products such as silica fume, FA, and SiMn slag, which are locally generated in significant quantities and are considered sustainable alternatives to traditional raw materials in meeting construction demands. Silica fume, produced in the smelting plant of Pertama Ferroalloys Sdn. Bhd. in Samalaju Industrial Zone, Bintulu, Sarawak, has an annual production of approximately 120,000 tons. It is categorized as scheduled waste under Malaysian regulations due to its high silica content (90.27% SiO_2). FA, a by-product of coal combustion in electric power plants, is another material utilized in this study. Malaysia has substantial coal reserves, estimated at approximately 1.9 billion MT, with 69% of these reserves located in Sarawak. FA is classified as scheduled waste and is produced in significant volumes from coal-based energy production (Usman Kankia et al., 2023). In addition, SiMn slag is produced as a by-product in the Samalaju Industrial Zone, with annual output ranging between 160,000 and 180,000 tons. This slag, also classified as scheduled waste, represents a considerable potential source of raw material for sustainable construction applications (Artika H et al., 2019). The properties of these materials utilized in this research are presented in Table 14.1.

The particle size distribution of FA, SiMn slag, SF, and fine sand is detailed in Fig. 14.2.

The Si/Al ratio is key to determining geopolymer concrete properties. A higher ratio enhances early strength, while a lower ratio improves corrosion resistance (Kucukgoncu & Özbayrak, 2024; Mustofa & Pintowantoro, 2016). Waterglass or sodium silicate supplies silica, and its concentration affects performance (Cong & Cheng, 2021). The optimal Si/Al ratio for balancing strength, especially with STF, is still debated and requires more research (Hanani Ismail et al., 2024). Calculating the Si/Al ratio involves determining the mass of silicon and aluminum from SiO_2 and Al_2O_3 percentages. The mass of Si was calculated from the percentage of SiO_2 using (14.1) (Ghita et al., 2011):

$$\text{Mass of Si} = \frac{\text{Mass of } SiO_2 \times \text{Ar(Si)}}{\text{Mr}(SiO_2)} \tag{14.1}$$

where Ar(Si) is the relative atomic mass of silicon (28.0855 g/mol) and Mr(SiO_2) is the molar mass of silicon dioxide (60.08 g/mol). Similarly, the mass of Al was derived from the percentage of Al_2O_3 using (14.2):

$$\text{Mass of Al} = \frac{\text{Mass of } Al_2O_3 \times 2 \times \text{Ar(Al)}}{\text{Mr}(Al_2O_3)} \tag{14.2}$$

where Ar(Al) is the relative atomic mass of aluminum (26.9815 g/mol) and Mr (Al_2O_3) is the molar mass of alumina (101.96 g/mol). Once the masses of Si and Al were calculated, the Si/Al ratio was determined by dividing the mass of Si by the mass of Al. To calculate the Si/Al ratio, first gather the mass and SiO_2 and Al_2O_3 percentages for each material are shown in Table 14.2. Sum the contributions of SiO_2 and Al_2O_3 to find their total content. Convert these totals to the masses of silicon (Si) and aluminum (Al) using molecular weight formulas. Divide the mass of Si by the mass of Al to determine the Si/Al ratio (Dinh et al., 2024), which is crucial for

Table 14.1 Materials properties used in this research.

Materials	Properties	Values
Class F fly ash, as per ASTM C 618, was obtained from the Sejingkat Coal-Fired Power Station in Kuching	Form	Powder
	Specific surface area	316 m²/kg
	Specific gravity	2.9.
	Particle size	19.22 μm
SiMn slag	Form	Rough and angular pieces
	Specific gravity	2.6
	Due to its irregular shape, the slag needed to be ground	<30 μm
	Specific surface area	509.341 m²/kg
Silica fume	Form	Ultrafine amorphous powder with a whitish-gray color
	Bulk density	150–700 kg/m³
	Specific gravity	2.1
	Particle size	0.4–0.5 μm
Fine sand used was river sand from Kuching	Particle sizes	Passing through a sieve of < 200 μm
	Specific surface area	236.429 m²/kg
	Fineness modulus	2.9
	Specific gravity	2.6
Steel fiber	Diameter	0.2 mm
	Length	13 mm
	Shape	A straight and plain
	specific gravity	7.86
Anhydrous sodium silicate (Na_2SiO_3) acted as the alkali activator	Specific gravity	2.61
	Molar mass	122.06 g/mol
Tap water	Used to mix these components, aiding in the hydration process, as well as regulating the consistency of the geopolymer concrete (Wei et al., 2020)	
Waterglass was a sodium silicate solution	Specific gravity	1.39
	Contain	Disodium metasilicate
	Total solids: %	45.46
	Baume @ 25°C	50
	Viscosity: Pa s	0.90
Superplasticizer	Used to improve the workability of the concrete mix without increasing the water content, which is crucial for achieving high density and reducing porosity (Memon et al., 2012).	

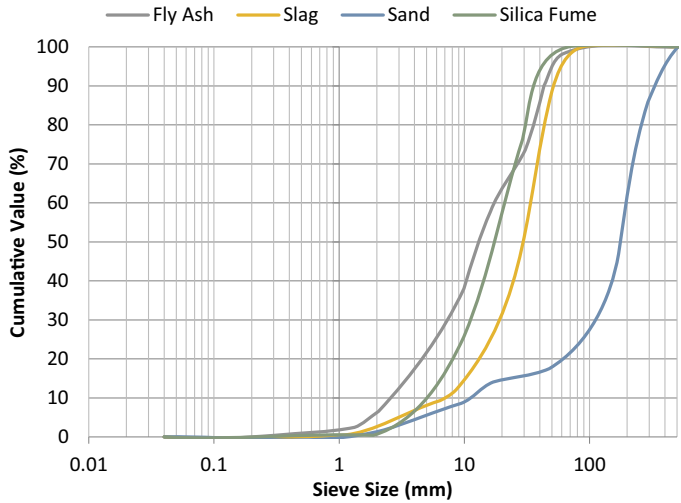

Figure 14.2 Size distribution of raw materials.

Table 14.2 Chemical composition of raw materials.

Chemical composition	FA	Slag	SF	Fine Sand	Na_2SiO_3 anhydrous	Waterglass
C	–	6.95	5.62	9.44	–	–
Na_2O	–	0.44	0.76	0.18	85	14.20
MgO	2.23	3.85	0.72	0.39	–	–
Al_2O_3	23.5	10.81	0.57	5.74	–	–
SiO_2	54.6	36.78	88.95	81.32	15	31.26
SO_3	0.79	1.3	–	–	–	–
K_2O	1.52	1.95	1.52	0.85	–	–
CaO	7.18	23.89	0.64	0.28	–	–
TiO_2	1.24	0.21	–	0.11	–	–
MnO	–	12.56	–	–	–	–
BaO	–	1.26	–	–	–	–
FeO	–	–	1.22	1.69	–	––
Fe_2O_3	8.1	–	–	–	–	–
P_2O_5	0.84	–	–	–	–	–

optimizing geopolymer concrete properties. Fig. 14.3 illustrates the detailed flowchart for calculating the Si/Al ratio.

FA, with high SiO_2 (54.6%) and Al_2O_3 (23.5%), is ideal for geopolymer formation due to its strong silica-alumina bonds. SiMn slag, with lower SiO_2 (36.78%) and

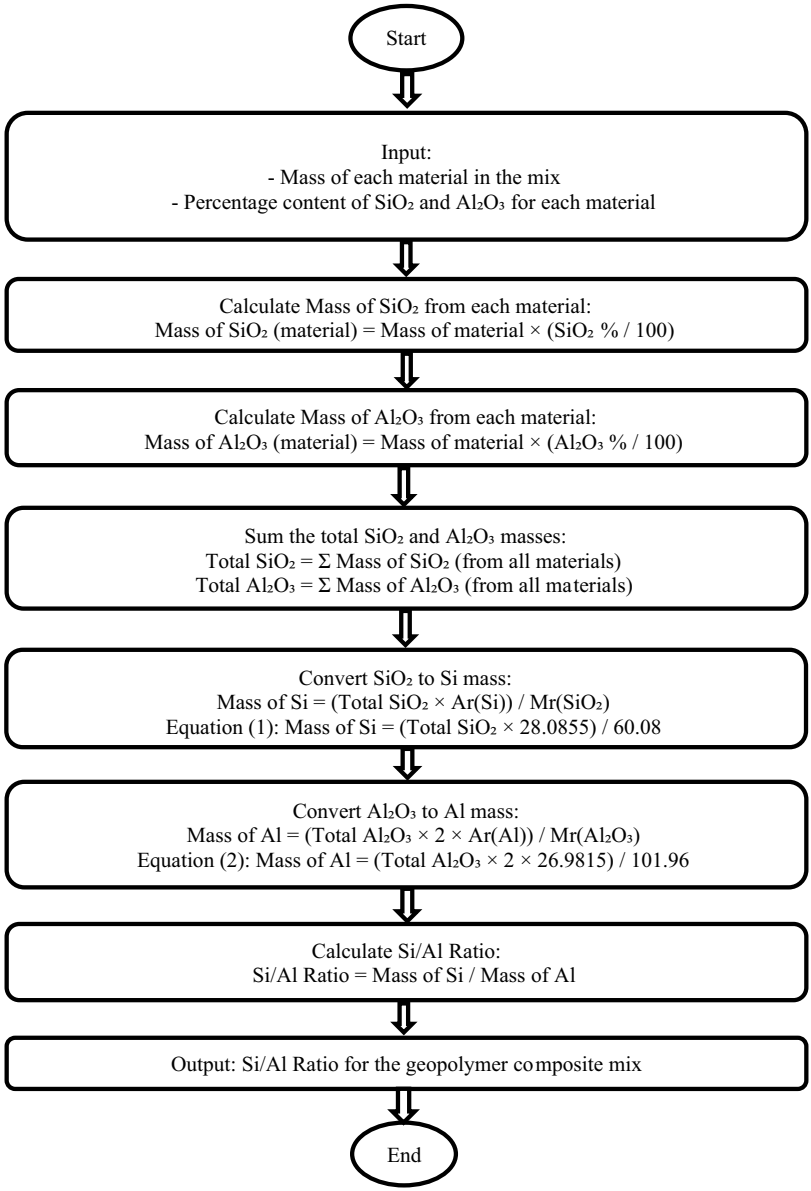

Figure 14.3 Flowchart calculation for Si/Al ratio.

Al_2O_3 (10.81%), also shows potential, especially when combined with other silica-rich materials. Using SiMn slag supports sustainability by repurposing industrial waste and reducing reliance on FA, which can be scarce or costly. This study explores SiMn slag's potential in creating innovative, eco-friendly geopolymer materials.

14.3.2 Geopolymer concrete production

The procedure began by preparing the alkali activator solution (AAS) by dissolving anhydrous Na_2SiO_3 in water and letting it cool for an hour. Precursors and aggregates were dry-mixed for 3 minutes at low speed (90 rpm), then combined with AAS and mixed for another 3 minutes. Fibers were added and mixed until uniformly distributed, followed by high-speed mixing (182 rpm) to eliminate fiber clumping. The mixture was cast into molds, compacted on a vibrating table for 2 minutes, and precured for 2 days at 27.3°C–29.6°C and 74.0%–92.0% humidity under plastic sheets. For optimal curing, samples were then heat-cured at 90°C for 48 hours, as high temperatures improve compressive strength (Verma Rao & Kumar, 2022). Castillo et al. (2021) stated that high moderate temperatures (80°C–90°C) induced higher compressive strengths in geopolymer, because the temperature favors the geopolymerization process (Castillo et al., 2021).

However, considering the primary aim of geopolymer concrete as a solution to reduce CO_2 emissions while achieving high compressive strength, previous studies have shown that using an oven at 90°C for 2 days can produce high compressive strength, exceeding 160 MPa (Lao et al., 2022). Samples were tested for compressive strength at 7, 14, and 28 days, with preparation details shown in Fig. 14.4.

14.3.3 Geopolymer concrete testing

For the compression test, concrete cubic specimens with a side length of 50 mm were designed according to Lao et al. (2022). The test samples were tested using a 2000-kN universal testing machine. The applied force ranged from 0 to 2000 kN and was tested at a loading rate of 0.6 MPa/s for compressive strength. In the flexural test on geopolymer concrete, beam specimens with dimensions of 50 mm × 50 mm × 200 mm are used. The standard test methods of ASTM C 293 were used to determine the flexural strength (Iqbal et al., 2024). The span length of the test specimen was divided into two portions, and the ratio of the straight distance between the point of load application and the nearest reaction to the depth of the beam was 1.5. In general, the span of the specimen was three times the depth.

14.3.4 Predictive modeling and data analytics

Machine learning models, such as those employed in geopolymer research, can predict material properties based on raw material characteristics and processing parameters. In geopolymer concrete, predictive models have been used to optimize mix designs by analyzing the effects of variables like FA content and activator concentration. For biocomposites, similar approaches can streamline the development process by reducing trial-and-error experimentation. Predictive modeling can help identify ideal fiber-matrix combinations and processing parameters, saving time and resources. For instance, data-driven simulations can predict how different fiber treatments or resin types will impact mechanical performance and durability, enabling rapid prototyping and optimization.

Figure 14.4 Steps for geopolymer concrete production.

Modeling techniques are key for optimizing geopolymer concrete composition (Rathnayaka et al., 2024). ANN, XGB, and MLR predict material properties based on chemical composition and ratios (Dang et al., 2024). ANN handles complex, nonlinear data (Huynh et al., 2020), XGB combines multiple models for accuracy (Cao et al., 2022), and MLR reveals linear relationships (Ahmed et al., 2022). Integrating these methods will help determine the optimal scheduled waste-based geopolymer concrete composition and Si/Al ratio. Accurate model specification is crucial for predicting ultra-high-strength lightweight geopolymer concrete (USLGPC) compressive strength. The regression equation links compressive strength to mix proportions, requiring careful determination of coefficients and handling multicollinearity. Validation ensures model accuracy, with least squares and matrix methods used for calculations. Cross-validation (CV) confirms robustness. The

coefficients $\beta_0, \ldots, \beta_8$ represent the effect of each variable on compressive strength, as shown in the multiple linear regression Eq. (14.3) (Schneider et al., 2010):

$$y_i = \beta_0 + \beta_1 x_{1i} + \beta_2 x_{2i} + \beta_p x_{pi} + \epsilon_i \tag{14.3}$$

where, y_i is the i^{th} observation of the dependent variable, x_{1i}, x_{pi} are the observations of the independent variables, β_0 is the intercept term, $\beta_1, \ldots, \beta_p$ are the coefficients to be estimated, and ε_i is the modeling error component of the i^{th} observation, also known as the residual. ANN models, like feedforward neural networks, are effective for regression tasks due to their simplicity and accuracy (Alamia et al., 2020). This study uses a multilayer perceptron (MLP) regressor to predict USLGPC compressive strength. The MLP includes an input layer, hidden layers for processing, and an output layer (Jain et al., 2015). Neurons are connected via weights, biases, and activation functions (Qamar & Ali Zardari, 2023), with activation described by Eq. (14.4):

$$\frac{1}{1 + e^{-A_j}} \tag{14.4}$$

where A_j is the value of the j^{th} neuron calculated as follows, Eq. (14.5):

$$A_j = \sum_{i=1}^{m} w_{ij} x_i + b_j \tag{14.5}$$

where w_{ij} is the weight between the j^{th} neuron and the previous layer, x_i denotes the i^{th} input, and b_j is the bias used to model the threshold. The final outputs are computed based on the calculated outputs of the hidden nodes as follows, Eqs. (14.6) and (14.7):

$$y_k = \frac{1}{1 + e^{-B_k}} \tag{14.6}$$

$$B_k = \sum_{j=1}^{m} w_{jk} y_j + b_k \tag{14.7}$$

where B_k is the activation of the k^{th} output node, w_{jk} is the connection weight from the j^{th} hidden node to the k^{th} output node, and b_k is the bias of the k^{th} output node. XGB is a gradient-boosting algorithm using decision trees as base learners. It improves prediction accuracy by sequentially updating residual errors and combining weak learners into a strong model, optimizing bias and variance (Chen & Guestrin, 2016). The prediction made by an XGB model is mathematically expressed in Eq. (14.8).

$$\hat{y}_i = \alpha \sum_{k=1}^{N} f_k(x_i) \tag{14.8}$$

where $\hat{y}_i$ is the predicted value, x_i is the input data with multiple features, α is the learning rate of the individual regression tree, N is the number of estimators, and f_k is the output of the k^{th} estimator. The quality of the obtained prediction results is evaluated via the objective function O expressed as follows, Eq. (14.9):

$$O = \sum_{i=1}^{n} L(y_i, \hat{y}_i) + \sum_{m=1}^{K} R(f_x) \tag{14.9}$$

where L is the loss function, representing the difference between y_i and $\hat{y}_i$. In addition, R is the regularization term that controls the complexity of the model and is defined as follows, Eq. (14.10):

$$R(f) = \gamma T + \frac{1}{2}\lambda \sum_{j=1}^{T} \omega_j^2 \tag{14.10}$$

where T is the total number of leaves of the regression trees, ω_j is the predicted value of the j^{th} leaf node, and γ and λ are the regularization parameters that control the magnitude of the weights assigned to the leaves and help prevent overfitting. The hyperparameters of XGB, such as the maximum tree depth ($d_{\max}$), the number of trees (estimators) N, the learning rate α, and the regularization parameters, γ and λ, can play an important role in the overall behavior and performance of the model. Therefore they normally require tuning (Chen & Guestrin, 2016). This study develops a model to predict the 28-day compressive strength of USLGPC using 190 data points from prior research and experiments. Mix proportions are the independent variables, and compressive strength is the dependent variable. MLR, XGB, ANN, and MLP regression models were trained to predict USLGPC compressive strength using 190 data points, including strengths over 100 MPa. Data was processed in Python (Joshi & Tiwari, 2023), split into training and testing sets, and evaluated with fivefold CV. ANN used 2 hidden layers, 10 neurons per layer, "relu" activation, "lbfgs" solver, alpha=0.1, and 3000 epochs. XGB's initial settings included max depth=3, learning rate=0.1, and 100 estimators, with hyperparameters later tuned using GridSearchCV. The maximum depth of the trees (d_max) was varied between 1 and 10, with a tolerance of 1. The regularization parameter α ranged from 0.1 to 0.2, with a tolerance of 0.02, while the number of boosting rounds (N) spanned values from 10 to 100, with a tolerance of 10. The minimum loss reduction required to make a further partition on a leaf node of the tree (γ) was set between 0.01 and 0.05, with a tolerance of 0.01. Lastly, the regularization parameter λ ranged from 0.1 to 1, with a tolerance of 0.1. These hyperparameters were systematically adjusted to fine-tune the model and improve prediction accuracy. A fivefold CV splits the data into five parts, using four for training and one for testing. Each model's performance was averaged across all folds and evaluated using R^2, Eq. (14.11).

$$R^2 = 1 - \frac{\sum_{i=1}^{n}(y_i - \hat{y}_i)^2}{\sum_{i=1}^{n}(y_i - \bar{y})^2} \tag{14.11}$$

where y_i is the actual value, $\hat{y}_i$ is the predicted one; $\bar{y}$ is the average of actual values, and n is the number of observations. The R^2 value measures how well the predictive model fits the actual data. It ranges between 0 and 1, with values closer to 1 indicating a better fit. Three models—ANN, XGB, and MLR—were developed to predict USLGPC compressive strength. ANN used an MLP architecture for nonlinear data, XGB applied boosting to reduce bias and variance, and MLR analyzed linear relationships. Model accuracy was validated with experimental data using mean squared error (MSE) and R^2 metrics. The design and modeling processes are shown in Figs. 14.5–14.7.

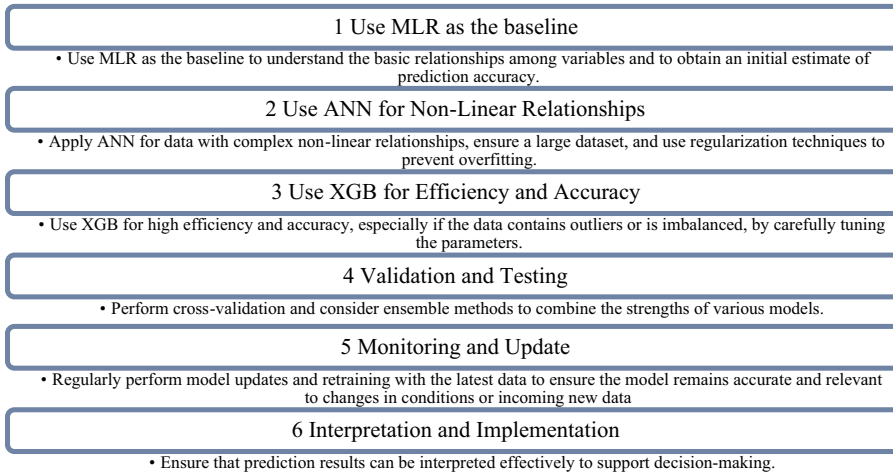

Figure 14.5 Design approach of the employed machine learning method.

14.3.5 Experiment design and model validation

To study USLGPC strength, 10 mixtures were designed using MLR, ANN, and XGB models. The best model guided the experiments. FA, SF, STF, and Na_2SiO_3 were kept constant, while varying SiMn slag, aggregates, waterglass, and water. Accuracy was validated by comparing experimental results with predictions using MSE, R^2, and residuals. Correlation analysis identified key relationships using coefficients and visualizations. Outliers were managed, and the data were split into training and testing sets for model building and evaluation. Coefficients showed positive correlations with SiMn slag, SF, fine aggregates, STF, Na_2SiO_3, waterglass, and water. Fig. 14.8 shows that multiple linear regressions prioritize the most influential materials.

14.3.6 Microscopic analysis

Microscopic analysis of geopolymer concrete used SEM and EDS to study its microstructure and chemical composition. SEM provided high-resolution images of surface morphology, while EDS detailed the elemental distribution. Samples were examined after 7, 14, and 28 days, with a platinum coating for conductivity. SEM and EDS, using a JEOL-JSM 6390A microscope, revealed how the Si/Al ratio and STF affected the concrete's internal structure (Wang et al., 2015). SEM images and EDS analysis of precursors and fine sand are shown in Fig. 14.9.

14.3.7 FTIR analysis

FTIR was used to identify chemical bonds and geopolymer phases, providing insights into functional groups and chemical stability. The analysis, performed with a Prestige21 Shimadzu system over a 400–4000 cm^{-1} range, using a DTGS KBr detector at 2 cm^{-1} resolution with 45 scans per sample. KBr disks were prepared by mixing

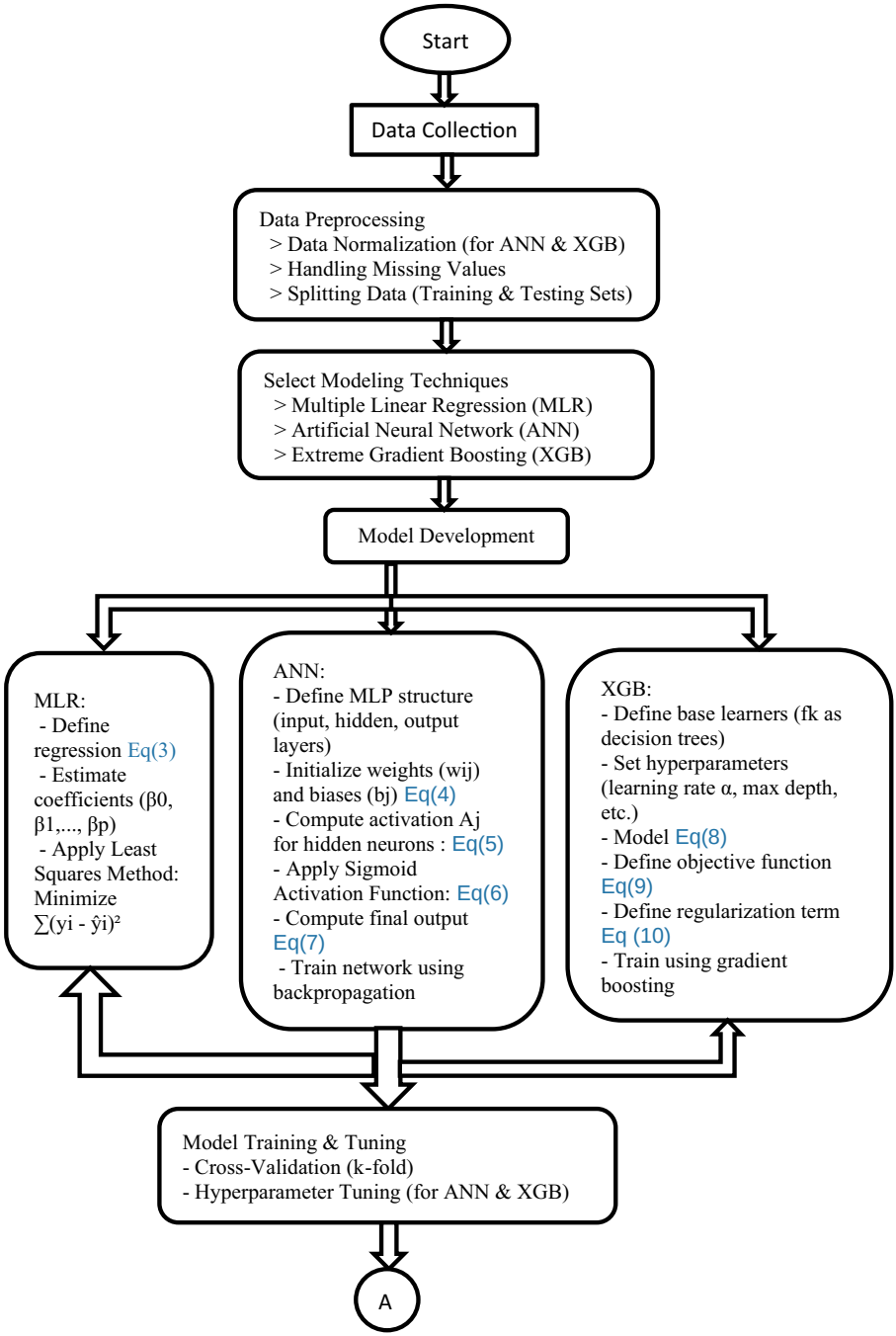

Figure 14.6 Flowchart for modeling prediction compressive strength of ultra-high-strength lightweight geopolymer concrete (*continued next*).

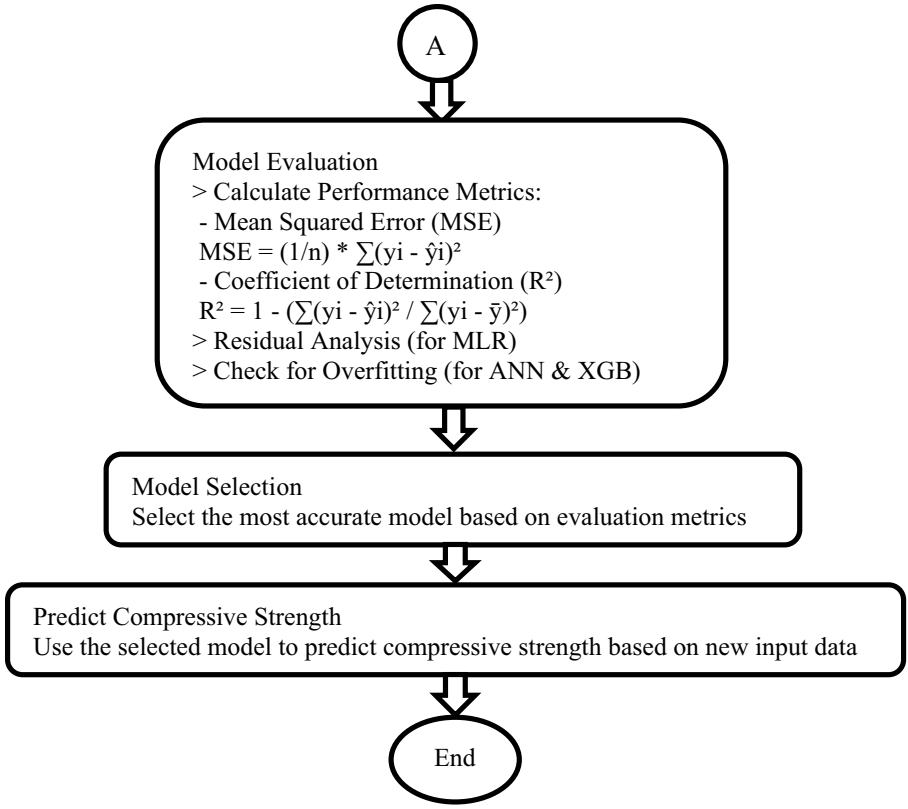

Figure 14.7 Flowchart for modeling prediction compressive strength of ultrahigh-strength lightweight geopolymer concrete.

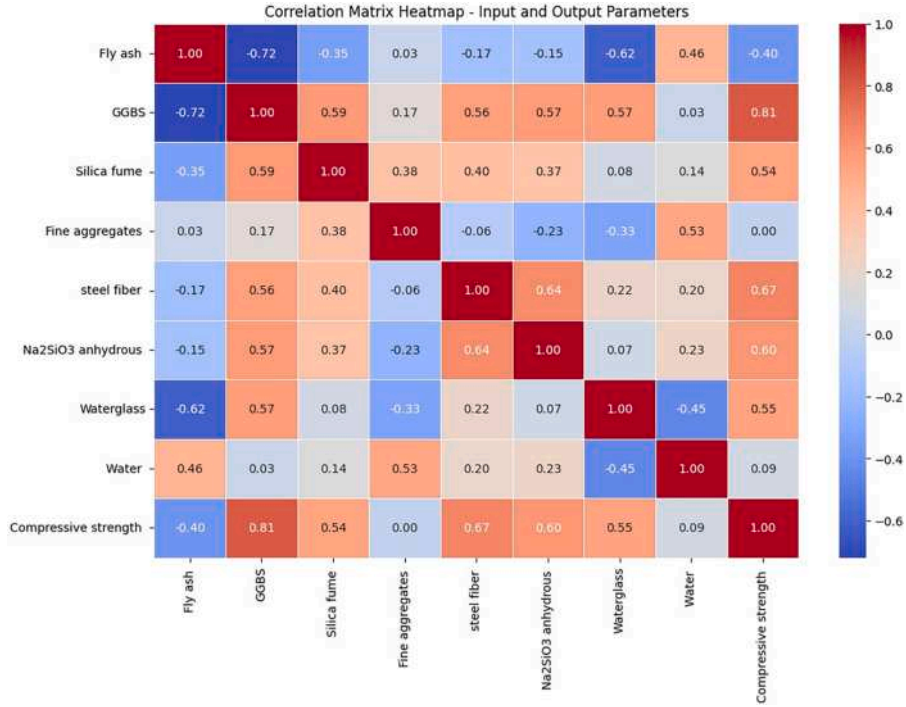

Figure 14.8 Heatmap data for the prediction model used.

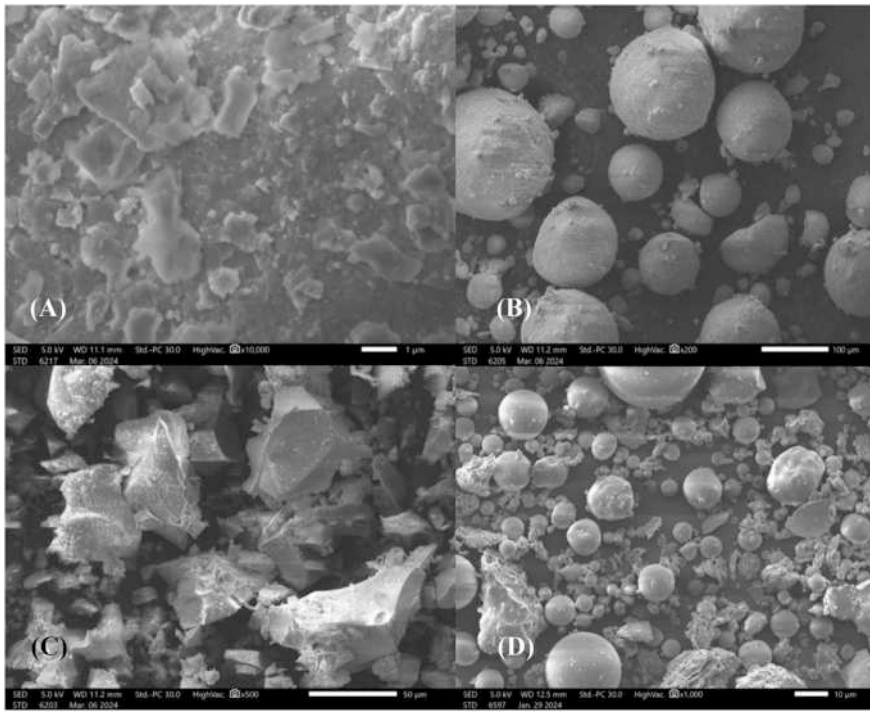

Figure 14.9 SEM images of raw materials (A) fine sand, (B) SF, (C) SiMn slag, and (D) FA.

2 mg of sample with 200 mg of KBr. The spectra were analyzed with IRsolution and Origin 9 software, focused on the 750–1300 cm^{-1} range for deconvolution using Gaussian peaks. Figs. 14.10 and 14.11 show FTIR images of materials in the USLGPC matrix, illustrating key chemical features and phases. FTIR analysis of FA reveals –OH groups at 3619.04 and 3438.62 cm^{-1}, high silicate content (1000–1100 cm^{-1}), and possible carbonates (1400–1600 cm^{-1}). These features suggest strong pozzolanic reactivity, beneficial for concrete strength. Further XRD analysis could confirm the mineral composition. The FTIR spectrum of sand shows high silica content with Si–O peaks at 1016 and 794 cm^{-1}, –OH groups and water around 3600–3200 and 1641 cm^{-1}, and minor carbonates at 1400 cm^{-1}. For SF, strong Si–O–Si peaks at 1100 and 800 cm^{-1} confirm its high silica content, with –OH groups and water indicated by peaks around 3400–3600 and 1641 cm^{-1}. Slag analysis reveals hydroxyl groups at 3435 cm^{-1}, Si–O–Si stretching between 1000 and 1100 cm^{-1}, carbonates around 1422–1448 cm^{-1}, and Si–O bending near 670–700 cm^{-1}, indicating a silicate-rich composition with possible carbonates.

14.3.8 Incorporating industrial by-products

Geopolymer concrete has successfully incorporated industrial by-products, such as FA and slag, to enhance sustainability and reduce costs. By utilizing these materials,

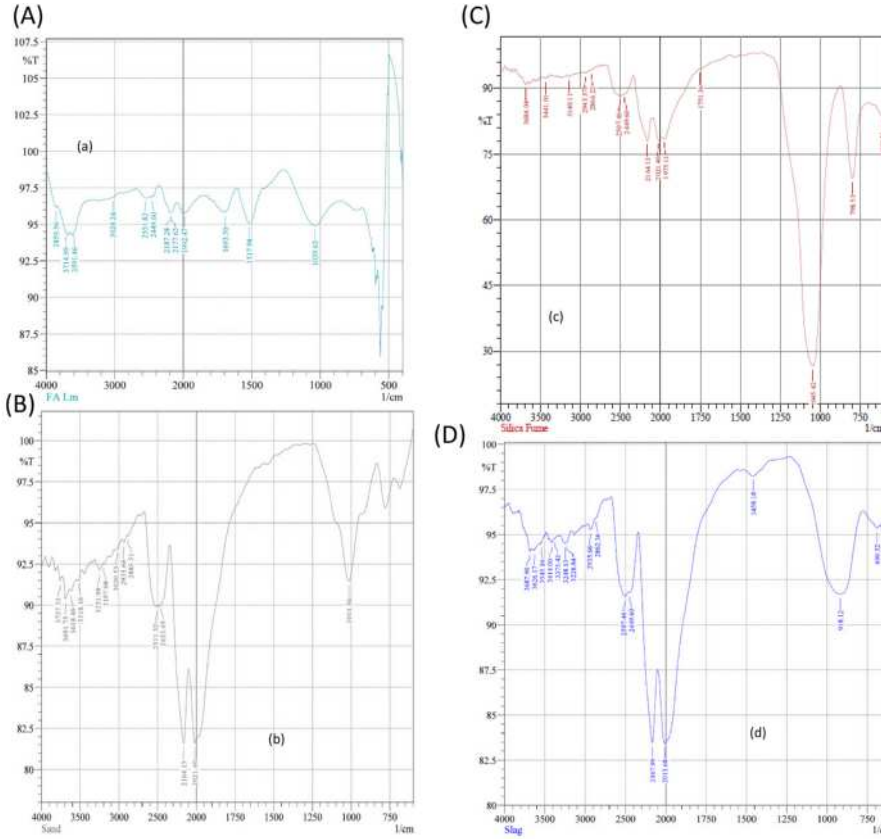

Figure 14.10 FTIR of raw materials: (A) FA, (B) fine sand, (C) Silica fume, and (D) Slag.

geopolymer concrete not only minimizes waste but also reduces reliance on energy-intensive raw materials like Portland cement. Similarly, biocomposites can leverage agricultural waste products, such as rice husk, coconut coir, and bagasse, to improve their environmental footprint. These by-products are abundant, renewable, and often discarded as waste, making them cost-effective alternatives to traditional fibers. For example, rice husk ash, rich in silica, can be combined with natural fibers to enhance the mechanical properties of biocomposites. Incorporating these by-products also supports circular economy principles by repurposing waste materials into valuable resources for sustainable manufacturing.

The performance of MLR, ANN, and XGB models was assessed using the R^2 measure. MLR achieved an R^2 of 0.85, while ANN and XGB showed superior performance with R^2 values of 0.911 and 0.938, respectively. The XGB model outperforms MLR and ANN based on performance metrics. It has the lowest MSE of 139.41, compared to ANN's 200.12 and MLR's 337.28, indicating superior prediction accuracy. XGB also leads with an R^2 of 0.938, surpassing ANN's 0.911 and MLR's 0.85, demonstrating the best variance explanation. Figs. 14.12 and 14.13 demonstrate

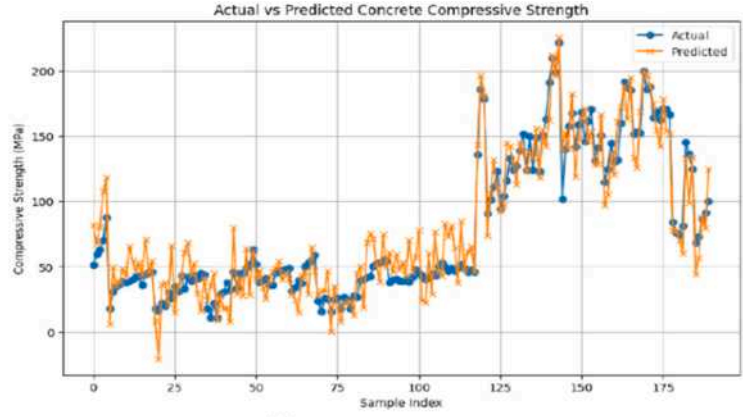

(A) Multiple Linear Regression

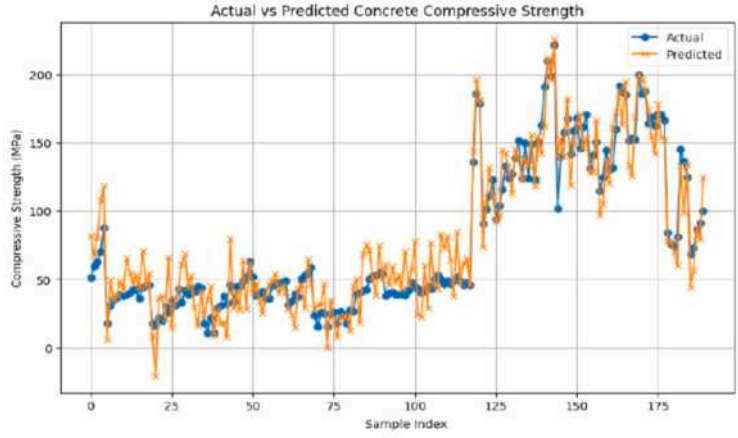

(B) Artificial Neural Network

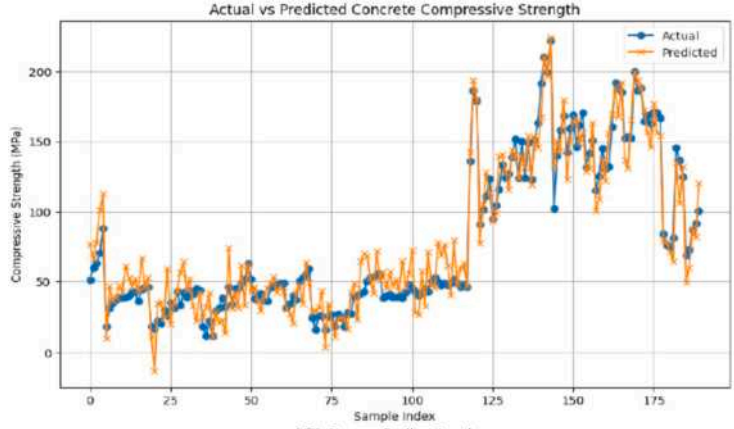

(C) Extreme Gradient Boosting

Figure 14.11 Comparison of actual and predicted concrete compressive strength.

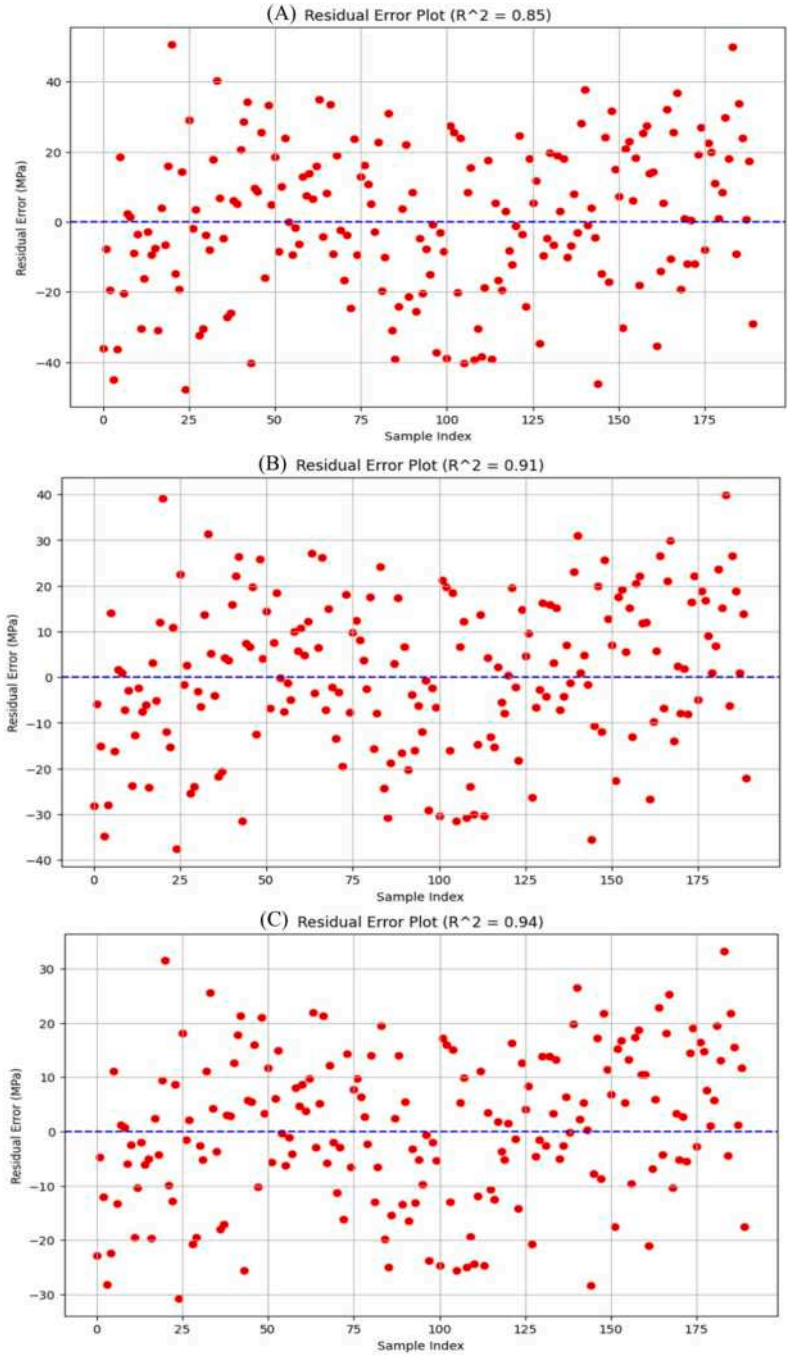

Figure 14.12 Comparison of predicted compressive strength and corresponding original values.

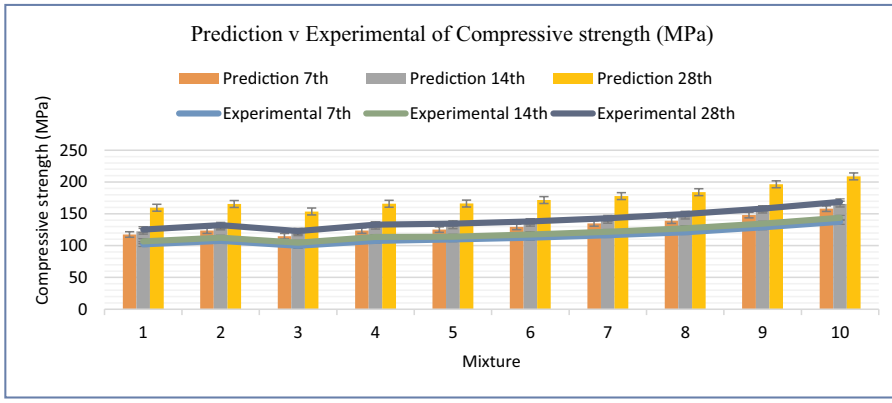

Figure 14.13 Plot of the residuals versus compressive strength for (A) MLR, (B) ANN, and (C) XGB models.

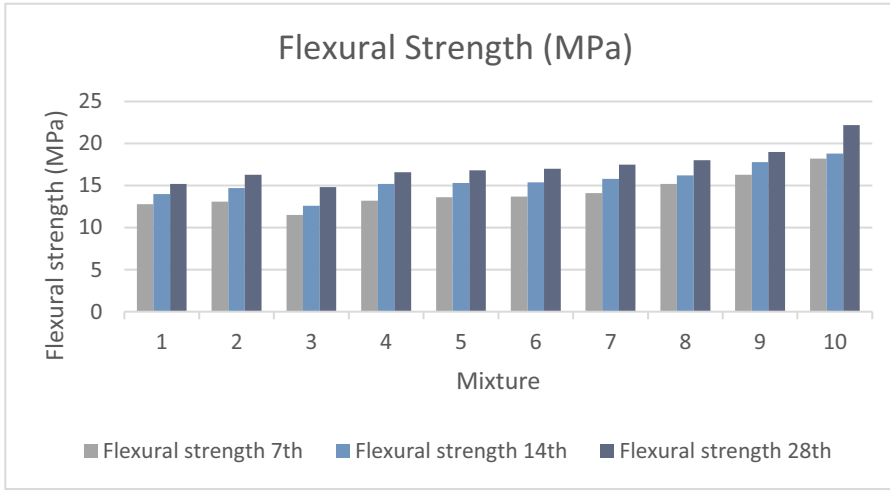

Figure 14.14 Comparison of the prediction and experimentally obtained compressive strength.

that although all models can predict USLGPC compressive strength, XGB and ANN significantly outperform MLR.

Fig. 14.14 compares predicted and experimental compressive strengths of USLGPC on days 7, 14, and 28. Mixtures 1–3 vary waterglass and water, mixtures 4–5 adjust fine sand, and mixtures 6–10 increase slag. Predicted strengths are 18%–22% higher than experimental values, within acceptable limits per Lewis's criteria (Van Dao et al., 2019). For mixtures 1–3, lower waterglass and water reduced strengths due to decreased binder effectiveness. Mixtures 4–5 showed that slight reductions in fine sand improved strengths, while mixtures 6–10 benefited from

increased slag content, supporting (Ahmad, Kontoleon, et al., 2022; Ahmad, Pu, et al., 2022) findings on GGBS's advantages over FA. Predictions were about 5%–10% lower than experimental results on day 7, increasing to 8%–12% by day 14, and widening to 12%–20% by day 28, with mixtures 4, 5, and 10 showing the largest discrepancies. Mixtures 1 and 6 had the smallest differences, within 5%. Overall, the models consistently underestimate strength by 5%–20%, indicating a need for refinement to improve long-term predictions.

Flexural strength test results show a clear increase from mixtures 1 to10, as illustrated in Fig. 14.15. By day 28, mixture 10, with the highest slag content, achieves 22.2 MPa, a 71% improvement over mixture 1. This strength increase is primarily due to the incorporation of STF and enhanced chemical bonding within the geopolymer matrix. STF improves ductility and crack resistance by bridging microcracks (Murali et al., 2024), allowing the concrete to absorb more energy. Additionally, the high slag content reacts with alkaline activators to create a robust matrix, strengthening over time. Mixtures 3–9 exhibit moderate flexural strengths (12–18 MPa), showing reliable designs but highlighting the need for optimized compositions. Overall, the results indicate that the strategic use of additives like slag and STF can significantly enhance flexural resistance, making these mixtures suitable for demanding applications.

Figs. 14.16 and 14.17 show SEM images of STF-reinforced geopolymer concrete after compression testing. The geopolymer remains strongly bonded to the STF, even when the fibers fracture. Fig. 14.18 shows SEM images of mixtures 1–3 with varying

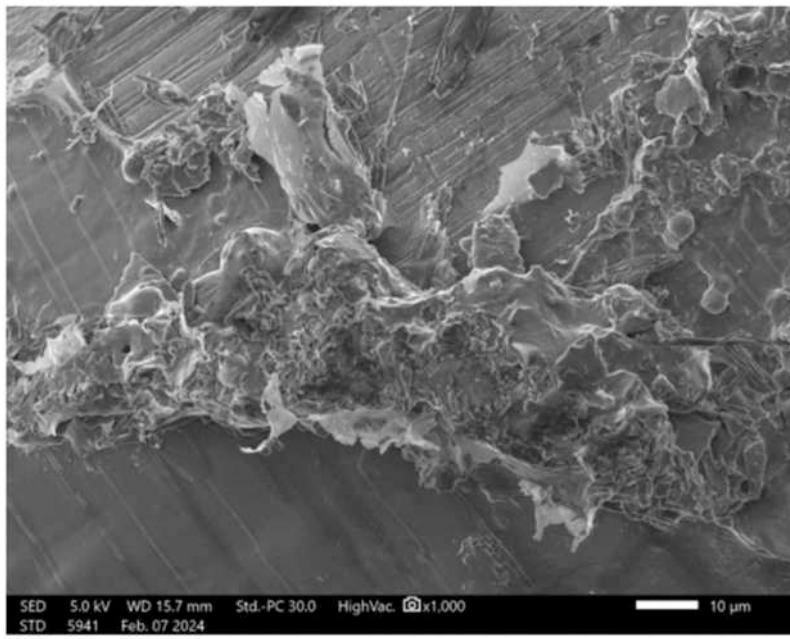

Figure 14.15 Flexural strength results.

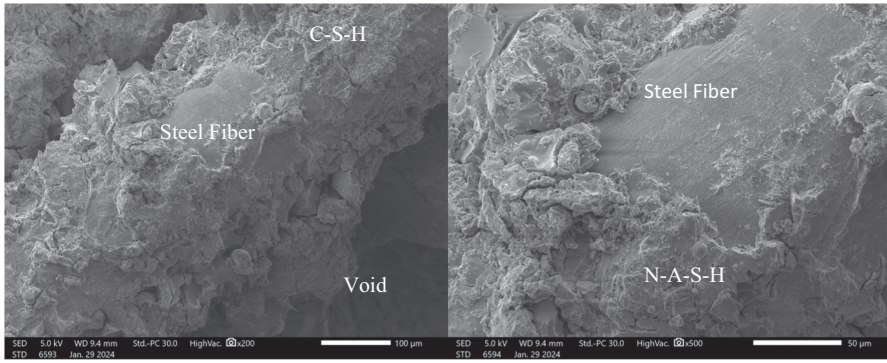

Figure 14.16 Geopolymer bonding on steel fiber.

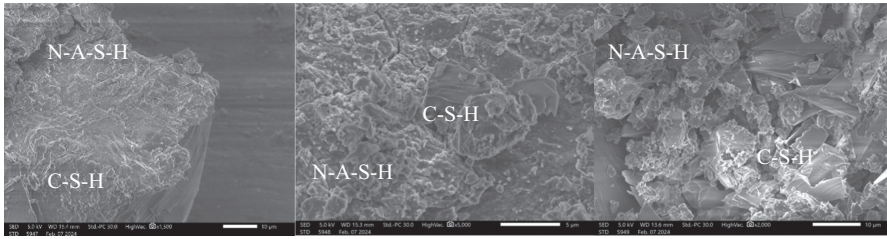

Figure 14.17 SEM images of STF-reinforced geopolymer concrete after compression test.

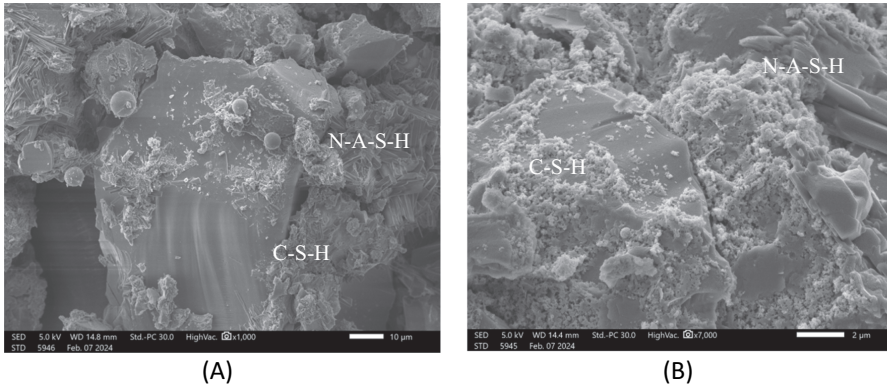

Figure 14.18 SEM images for (A) mixture 1, (B) mixture 2, and (C) mixture 3.

waterglass and water reductions. Mixture 1, with a 12.5% reduction, has noticeable gaps and porosity from unreacted materials. As stated by Siddika et al. (2021), unreacted materials optimally tend to form porosity, which can reduce density. Mixture 2, using predicted amounts, showed fewer gaps and better material reaction.

Mixture 3, with a 25% reduction, has more gaps due to insufficient alkali activator and incomplete material reaction.

Fig. 14.19 shows SEM images of mixtures 4 and 5 with 8% and 16% reductions in fine sand from the predicted amounts. Less fine sand leads to more geopolymer bonds as the binder focuses on other materials, making the concrete stickier. According to Amran et al. (2021), less fine sand allows for better binding and fewer gaps, thus enhancing compressive strength. Fig. 14.20 shows SEM images of mixtures 6 to 10 with increasing slag amounts: 8%, 16%, 23%, 38%, and 54%. More slag enhances geopolymer bond formation due to higher alumina content, which binds more effectively with silica from the alkali activator, closing gaps and improving compressive strength. STF further reinforces the matrix. EDS analysis identifies calcium (Ca), silicon (Si), sodium (Na), aluminum (Al), and oxygen (O), indicating the presence of both C–S–H and N–A–S–H gels Qaidi, Najm, et al. (2022), though distinguishing between them morphologically is challenging.

The FTIR spectrum is used to identify the chemical compounds formed in geopolymer concrete and to evaluate the chemical stability of the composite. Fig. 14.21 presents the FTIR spectra for geopolymer concrete with varying Si/Al ratios. The main peaks identified include Si–O–Si, Si–O–Al, and OH bonds. At the optimal Si/Al ratio, the spectrum shows strong peaks between 950–1100 cm^{-1}, indicating the efficient formation of the geopolymer network. According to Delgado-Plana et al. (2021), observed that the Si–O–T (T:Si or Al) stretching vibration, centered on the precursor at 1035 cm^{-1}, shifted to lower frequencies in the geopolymers (1004–994 cm^{-1}).

The change in geopolymer structure indicates successful geopolymerization, forming N–A–S–H gel. A lower Si/Al ratio introduces new peaks at 1009.63 cm^{-1}, linked to Si–O vibrations and the formation of amorphous aluminosilicate and zeolite

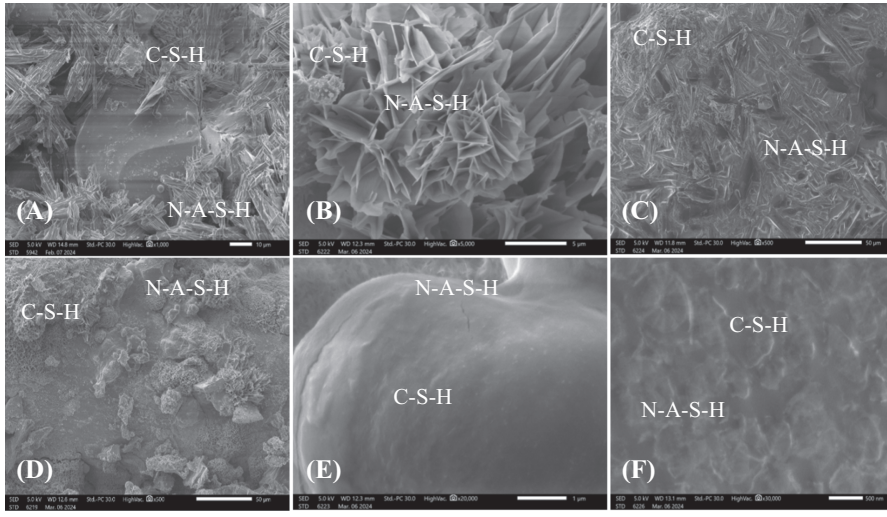

Figure 14.19 SEM images for (A) mixture 4 and (B) mixture 5.

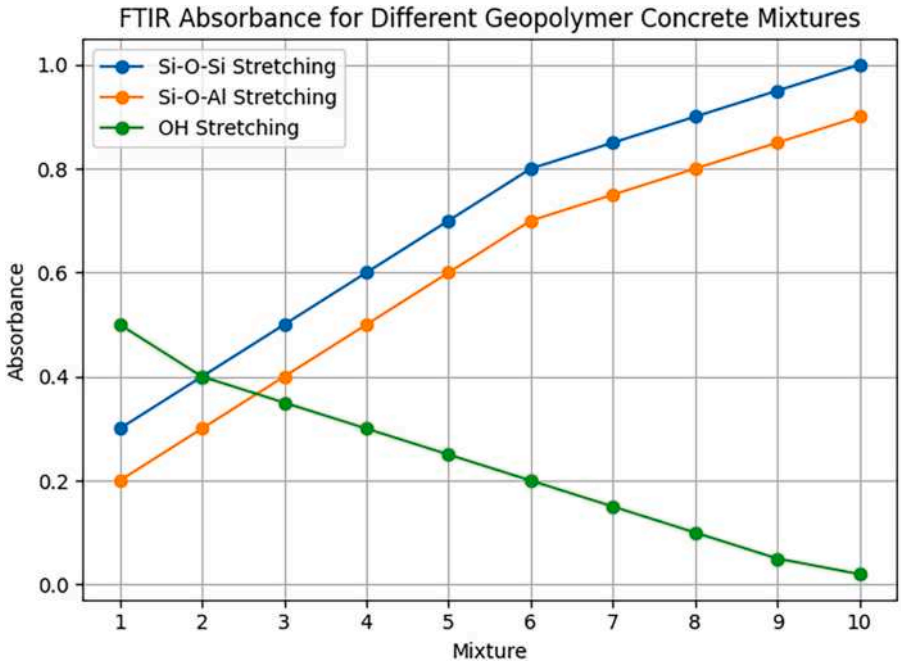

Figure 14.20 SEM images for (A) mixture 6, (B) mixture 6, (C) mixture 7, (D) mixture 8, (E) mixture 9, and (F) mixture 10.

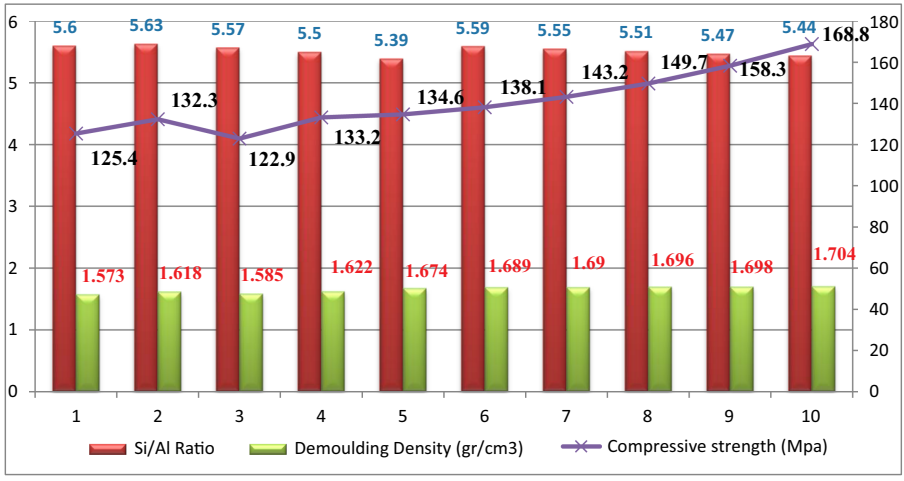

Figure 14.21 FTIR spectra for geopolymer concrete with varying mixtures.

phases. Higher Si/Al ratios show more amorphous phases, which may reduce stability (Cui et al., 2023). In mixtures 1–3, weak Si–O–Si and Si–O–Al peaks correlate with lower compressive strength. In contrast, mixtures 4–5 exhibit improved peak intensity, reflecting enhanced geopolymer network formation and increased strength. Furthermore, mixtures 6–10 demonstrate that increased slag boosts Si–O peaks, indicating a strong and stable network with low moisture content, thereby supporting optimal compressive strength.

14.3.9 Influence of the silica-alumina ratio on concrete strength

Table 14.3 presents the mix compositions, while Table 14.4 highlights the relationship between the Si/Al ratio, demolding density, and compressive strength in ten geopolymer mixtures.

Fig. 14.22 relationship between Si/Al ratio, experimental compressive strength (MPa), and demoulding density (g/cm^3).

Lower Si/Al ratios correlate with increased compressive strength and denser microstructures. Mixtures 1–3 (Si/Al ratios of 5.57–5.63) achieve compressive strengths of 122.9–132.3 MPa but are closer to lightweight concrete properties (1.573–1.618 g/cm³). Mixtures 4 and 5 (Si/Al ratios of 5.5 and 5.39) show improved strengths (133.2–134.6 MPa) with higher densities (1.622–1.674 g/cm³). Mixtures 6–10, with Si/Al ratios of 5.59–5.44, reach a peak strength of 168.8 MPa at a density of 1.704 g/cm³, but are further from lightweight goals. Overall, optimizing Si/Al ratios below 5.5 enhances strength while increasing density, indicating a trade-off for lightweight applications. Higher density mixtures, like mixture 10, show better strength due to reduced porosity. Conventional concrete has strengths of 20–60 MPa and densities of 2200–2600 kg/m³. Lightweight concrete uses lower specific gravity materials to reduce density while maintaining strength, but it often has lower mechanical properties

Table 14.3 Mix composition for ultrahigh-strength lightweight geopolymer concrete experimental.

Mix proportion by weight	Mixture no.									
	1	**2**	**3**	**4**	**5**	**6**	**7**	**8**	**9**	**10**
Na_2SiO_3 (anhydrous)	1.00	1.00	1.00	1.00	1.00	1.00	1.00	1.00	1.00	1.00
Fly ash	2.50	2.50	2.50	2.50	2.50	2.50	2.50	2.50	2.50	2.50
SiMn Slag	7.00	7.00	7.00	7.00	7.00	7.25	7.50	7.75	8.00	8.20
Silica fume	1.50	1.50	1.50	1.50	1.50	1.50	1.50	1.50	1.50	1.50
Waterglass	1.75	2.00	1.50	2.00	2.00	2.00	2.00	2.00	2.00	2.00
Water	1.21	1.21	0.90	1.21	1.21	1.24	1.21	1.21	1.20	1.22
Fine sand	6.05	6.05	6.05	5.50	5.06	6.02	6.04	6.05	6.00	6.04
Steel fiber	1.57	1.57	1.57	1.57	1.57	1.57	1.57	1.57	1.57	1.57

Table 14.4 Total SiO_2 and Al_2O_3 forming the Si/Al ratio.

Mixture	Total mass SiO_2	Total mass Al_2O_3	Mass of Si	Mass of Al	Si/Al ratio	Demoulding density (gr/cm^3)	Compressive strength (Mpa)	Remarks
1	1078.12	170.002	503.99	89.97	5.60	1.573	125.4	High Si/Al ratios in mixtures 1–3 reduce compressive strength, indicating that ratios above 5.5 are suboptimal. Lower densities weaken the geopolymer network, suggesting that reducing the Si/Al ratio and increasing density could improve performance.
2	1084.37	170.002	506.91	89.97	5.63	1.618	132.3	
3	1071.87	170.002	501.07	89.97	5.57	1.585	122.9	
4	1039.65	166.845	486.00	88.30	5.50	1.622	133.2	Mixtures 4 and 5 indicate that reducing the Si/Al ratio below 5.5 improves compressive strength. Mixture 5, with a ratio of 5.39 and a density of 1.674 g/cm³, shows enhanced strength, suggesting that further lowering the Si/Al ratio and increasing density could yield even better results.
5	1003.86	164.319	469.27	86.97	5.39	1.674	134.6	
6	1091.13	172.532	510.07	91.31	5.59	1.689	138.1	Mixtures 6 and 7 demonstrate improved compressive strength, with Mixture 7 reaching 143.2 MPa at a Si/Al ratio of 5.55. The increased demoulding density enhances the geopolymer network, suggesting that optimizing the Si/Al ratio and density boosts performance, making these mixtures suitable for high-strength applications.
7	1101.95	175.349	515.13	92.80	5.55	1.690	143.2	
8	1111.96	178.109	519.80	94.27	5.51	1.696	149.7	Mixtures 8–10 show increased compressive strength as Si/Al ratios fall below 5.5. Mixture 10, with a ratio of 5.44 and density of 1.704 g/cm³, achieves the highest strength of 168.8 MPa, highlighting the benefit of lowering the Si/Al ratio and maximizing density for optimal performance.
9	1117.09	180.525	522.20	95.54	5.47	1.698	158.3	
10	1127.69	182.917	527.16	96.81	5.44	1.704	168.8	

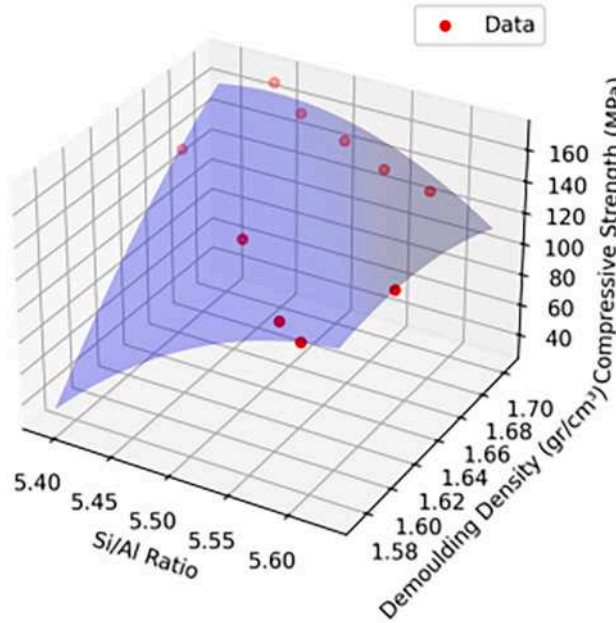

Figure 14.22 Correlation between Si/Al ratio, demoulding density, and compressive strength.

and increased brittleness. Optimizing the Si/Al ratio and density is essential to balance strength and lightweight requirements for specific applications.

Fig. 14.23 shows a strong negative Pearson correlation coefficient of -0.897 between the Si/Al ratio and compressive strength, with a *P* value of .0004. This indicates that lower Si/Al ratios significantly increase compressive strength, and the correlation is statistically significant. However, further research with a broader range of Si/Al ratios is needed to determine accurate lower and upper limits, enhancing our understanding of their impact on concrete strength.

14.3.10 Production cost analysis

The cost evaluation reveals that optimizing the Si/Al ratio enhances concrete strength while significantly reducing production costs. The use of scheduled wastes, a lower-cost industrial by-product, is key to this cost reduction. Mixtures with a moderate Si/Al ratio strike the best balance between cost and strength, as they require less sodium silicate and more waterglass, directly lowering costs. While adding STF improves flexural strength, it also increases costs. Tables 14.5 and 14.6 provide a detailed cost analysis of producing 1 m³ of concrete, comparing various types with similar 28-day compressive strengths from prior studies and experiments in this research, using Malaysian currency.

Fig. 14.24 shows a trade-off between compressive strength and cost across mixtures. Mixture 10 achieves the highest strength (168.8 MPa) but at a cost of RM 72,134.2/m^3,

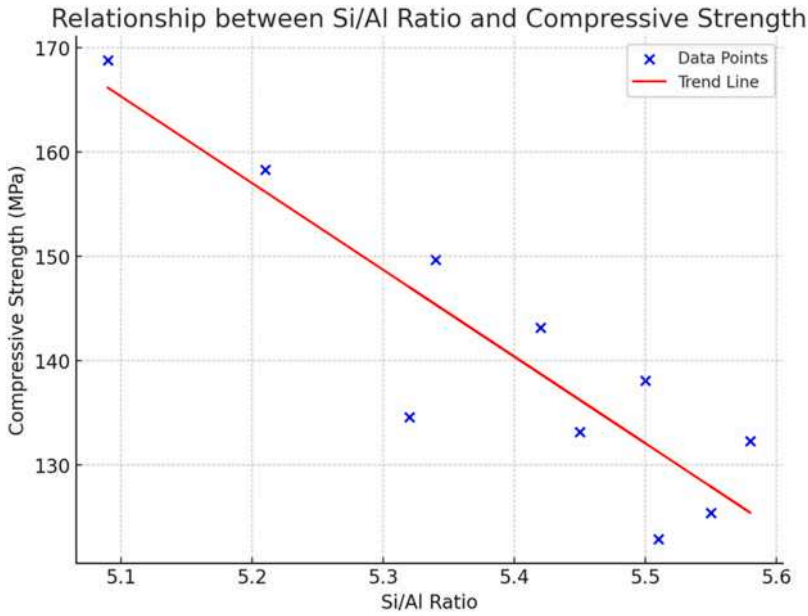

Figure 14.23 Correlation between Si/Al ratio and compressive strength.

making it suitable for projects prioritizing performance over budget. Compared to Saleem et al. (2024), whose UHPC mix reached 162 MPa using a high amount of cement, mixture 10 offers similar strength without cement, highlighting its sustainability. However, mixture 10 is 293.3% more expensive than Saleem's UHPC. SH-UHPGC mixtures also show rising costs with strength, with SH-UHPGC 2 (186 MPa) at RM 67,129.99 and SH-UHPGC 3 (179 MPa) at RM 72,739.99. Despite some SH-UHPGC mixes achieving higher strengths, the experimental mixtures (RM 71,608.7–RM 72,134.7) show a consistent cost-to-performance ratio, making them a cost-effective alternative, especially considering material availability.

SH-UHPGC and USLGPC are the most cost-effective options, offering high strength at lower costs than conventional high-strength concrete. Despite the use of expensive materials like sodium silicate and STF, the use of industrial waste and optimized Si/Al ratios significantly reduces costs. For example, sodium silicate in Mixture 6 accounts for RM 55,550 of the total RM 72,134.7, with STF adding RM 15,000. Reducing costs can be achieved by replacing these with cheaper alternatives, such as synthetic or natural fibers and affordable alkaline activators. This could make USLGPC a more competitive, sustainable alternative to traditional concrete.

14.3.11 Environmental sustainability

Geopolymer concrete, when optimized for a high Si/Al ratio, significantly reduces the environmental impact of construction compared to traditional Portland cement, which is a major source of CO_2 emissions. By using GGBS, FA, or other waste materials,

Table 14.5 Cost analysis for concrete 1 m^3 production based on previous studies.

Materials	Cost (RM/kg)					Lao et al. (2023)						Lao et al (2022)					
		UHPC-SCBA	Cost	UHPC	Cost	SH-UHPGC 1	Cost	SH-UHPGC 2	Cost	SH-UHPGC 3	Cost	UHPGC 1	Cost	UHPGC 2	Cost	UHPGC 3	Cost
Cement	0.46	1212.9	558.904	800	368.64	–	–	–	–	–	–	–	–	–	–	–	–
Fine sand	0.0485	–	–	430	20.834	–	–	–	–	–	–	691.5	33.503	699.0	33.867	706.8	34.244
Silica sand	2.0	–	–	430	855.7	675	1343.25	675	1343.25	675	1343.25	–	–	–	–	–	–
SF	0.01	282.8	2.828	233	2.33	80	0.80	80	0.80	80	0.80	81.9	0.819	82.8	0.828	83.7	0.837
Quartz sand	0.3	615.1	172.0	–	–	–	–	–	–	–	–	–	–	–	–	–	–
Quartz powder	1.1	72.8	81.9	210	236.25	–	–	–	–	–	–	–	–	–	–	–	–
Superplasticizer	40.0	37.4	1496	42.5	1700	–	–	–	–	–	–	–	–	–	–	–	–
Steel fibers	100.0	–	–	150	15000	156	15600	156	15600	156	15600	237.2	23720	237.3	23730	237.3	23730
Water	0.76	254.7	193.58	207	157.32	186	141.36	186	141.36	186	141.36	103.4	78.584	104.6	79.496	105.7	80.332
FA	0.01	–	–	–	–	192	1.92	192	1.92	192	1.92	589.1	5.891	397.0	3.970	200.7	2.007
Sodium silicate	550.0	–	–	–	–	–	–	49.3	27115	98.5	54175	101.0	55550	102.1	56155	103.2	56760
Slag	0.01	–	–	–	–	766	7.66	766	7.66	766	7.66	392.7	3.927	595.6	5.956	802.9	8.029
Waterglass	10.0	–	–	–	–	147	1470	147	1470	147	1470	150.4	1504	152.1	1521	153.8	1538
Borax	200.0	–	–	–	–	–	–	–	–	–	–	50.5	10100	51.0	10200	51.6	10320
Sodium carbonate	500.0	–	–	–	–	85.6	42800	42.9	21450	–	–	–	–	–	–	–	–
SCBA	0.514	109.2	56.129	–	–	–	–	–	–	–	–	–	–	–	–	–	–
Total cost for 1 m3 (RM)		2561.341		18,341.074		61,364.990		67,129.99		72,739.990		90996.724		91730.117		92473.449	
Compressive strength at 28 days (Mpa)		133		162		135.8		186		179		163		191		210	

SCBA, Sugarcane bagasse ash.

Table 14.6 Cost analysis for concrete 1 m^3 production in this study.

Materials	Cost (RM/kg)	Experiment																			
		Mixture 1	Cost	Mixture 2	Cost	Mixture 3	Cost	Mixture 4	Cost	Mixture 5	Cost	Mixture 6	Cost	Mixture 7	Cost	Mixture 8	Cost	Mixture 9	Cost	Mixture 10	Cost
Cement	0.46	–	–	–	–	–	–	–	–	–	–	–	–	–	–	–	–	–	–	–	–
Fine sand	0.0485	605	29.31	605	29.312	605	29.31	550	26.647	506	24.515	602	29.16	604	29.26	605	29.31	600	29.07	604	29.26
Silica sand	2.0	–	0	–	–	–	–	–	–	–	–	–	–	–	–	–	–	–	–	–	–
Silica Fume	0.01	150	1.5	150	1.5	150	1.5	150	1.5	150	1.5	150	1.5	150	1.5	150	1.5	150	1.5	150	1.5
Quartz sand	0.3	–	0	–	–	–	–	–	–	–	–	–	–	–	–	–	–	–	–	–	–
Quartz powder	1.1	–	0	–	–	–	–	–	–	–	–	–	–	–	–	–	–	–	–	–	–
Superplasticizer	40.0	–	0	–	–	–	–	–	–	–	–	–	–	–	–	–	–	–	–	–	–
Steel fibers	100.0	150	15,000	150	15,000	150	15,000	150	15,000	150	15,000	150	15,000	150	15,000	150	15000	150	15000	150	15000
Water	0.76	121	91.96	121	91.96	90	68.4	121	91.96	121	91.96	124	94.24	121	91.96	121	91.96	120	91.2	122	92.72
FA	0.01	250	2.5	250	2.5	250	2.5	250	2.5	250	2.5	250	2.5	250	2.5	250	2.5	250	2.5	250	2.5
Sodium silicate	550.0	100	55,000	100	55,000	100	55,000	100	55,000	100	55,000	100	55,000	100	55,000	100	55000	100	55000	100	55000
Slag	0.01	700	7	700	7	700	7	700	7	700	7	725	7.25	750	7.5	775	7.75	800	8	820	8.2
Waterglass	10.0	175	1750	200	2000	150	1500	200	2000	200	2000	200	2000	200	2000	200	2000	200	2000	200	2000
Borax	200.0	–	0	–	–	–	–	–	–	–	–	–	–	–	–	–	–	–	–	–	–
Sodium carbonate	500.0	–	0	–	–	–	–	–	–	–	–	–	–	–	–	–	–	–	–	–	–
SCBA	0.514	–	0	–	–	–	–	–	–	–	–	–	–	–	–	–	–	–	–	–	–
Total cost for 1 m3 (RM)		71,882.27		72,132.3		71,608.7		72,129.6		72,127.5		72,134.7		72,132.7		72,131.6		72132.3		72134.2	
Compressive strength at 28 days (MPa)		125.4		132.3		122.9		133.2		134.6		138.1		143.2		149.7		158.3		168.8	

SCBA, Sugarcane bagasse ash.

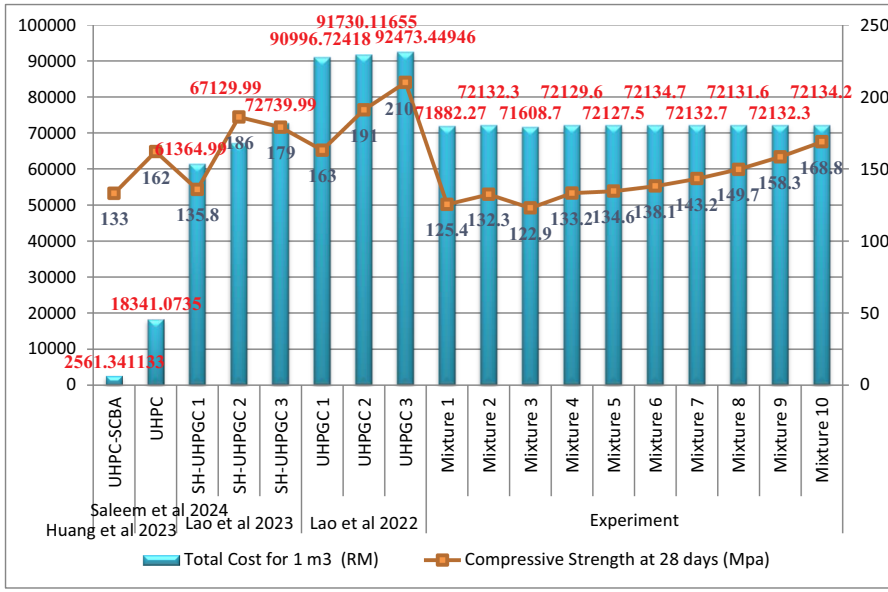

Figure 14.24 Comparison of cost analysis for different types of concrete.

and with a high Si/Al ratio, the production process can incorporate a larger amount of waste materials, reducing reliance on virgin resources and avoiding the carbon-intensive calcination process, leading to lower emissions. An optimized Si/Al ratio also results in longer-lasting structures that require less maintenance, conserving energy and materials over time. Lightweight geopolymer concrete further adds sustainability benefits by reducing raw material use and lowering energy consumption in buildings. The integration of recycled aggregates enhances its environmental profile, making it an eco-friendly option for sustainable construction. In summary, with a high Si/Al ratio and large-scale use of waste materials, geopolymer concrete combines high performance with economic and environmental advantages, offering a sustainable solution for the construction industry.

The study on USLGPC, optimizing the Si/Al ratio with SiMn slag, advanced modeling, and cost analysis, revealed key findings. The XGB model performed best, with an MSE of 139.41 and R^2 of 0.938, outperforming ANN (MSE 200.12, R^2 0.911) and MLR (MSE 337.28, R^2 0.85). Predicted compressive strengths were 18%–22% higher than experimental results. The highest flexural strength of 22.2 MPa, a 71% increase from mixture 1, was due to STF and optimized geopolymer chemistry. SEM analysis showed strong adhesion and reduced porosity with higher slag content. FTIR confirmed that optimal Si/Al ratios improved geopolymer network strength, while lower ratios led to amorphous phases. Compressive strength improved with reduced Si/Al ratios and higher SiO_2 and Al_2O_3 masses—a density of 1.704 g/cm³, balanced lightweight design, and strength. Costs ranged from RM71,608.7 to RM72,134.7/m^3, with strengths of 122.9–168.8 MPa. The study highlights the economic and

performance benefits of optimized Si/Al ratios and selective STF use in USLGPC for sustainable construction.

14.4 Future directions

14.4.1 Innovations in material sourcing

Biocomposite development must prioritize novel natural fibers and innovative resins to enhance material performance and sustainability. Algae- and fungi-based fibers, for example, offer high growth rates, low environmental impact, and unique mechanical properties such as flexibility and durability. These sources are also less dependent on arable land, making them a viable alternative to traditional crops. Additionally, advanced bio-based resins, such as those derived from lignin or cellulose, exhibit improved thermal and mechanical stability, enabling biocomposites to compete in high-performance applications. Research into these materials can lead to breakthroughs in both cost efficiency and ecological benefits.

14.4.2 Hybrid biocomposites

Combining natural fibers with synthetic or nano-reinforcements presents an opportunity to achieve superior mechanical performance while maintaining sustainability. Hybrid composites, such as those integrating carbon nanotubes or graphene with natural fibers, offer enhanced tensile strength, elasticity, and thermal conductivity. Similarly, hybrid matrices that combine bio-based polymers with conventional resins can optimize cost and performance. Investigating the synergistic effects of these combinations through experimental studies and computational modeling will be critical in advancing hybrid biocomposite technologies.

14.4.3 Advanced processing techniques

Investing in state-of-the-art processing technologies is essential for improving the quality and scalability of biocomposites. Additive manufacturing, such as 3D printing, allows for precision fabrication and reduced material waste, making it ideal for customized applications. Automated fiber placement techniques can enhance production efficiency and consistency, particularly for large-scale components. Furthermore, eco-friendly pretreatment methods, such as enzymatic treatments or supercritical CO_2 processing, can improve fiber-matrix adhesion without harmful chemicals, supporting both performance and environmental goals.

14.4.4 Economic feasibility

Achieving economic viability for biocomposites requires comprehensive cost-benefit analyses to identify the most efficient production pathways. Policymakers can incentivize biocomposite adoption through subsidies, tax breaks, and grants for sustainable materials. Partnerships with industries, such as the automotive and construction sectors, can facilitate the integration of biocomposites into existing

supply chains, reducing market entry barriers. Scaling up production with shared resources and infrastructure can also significantly lower costs.

14.4.5 Comprehensive life cycle analysis

Performing detailed LCAs is essential to quantify the environmental and economic impacts of biocomposites from cradle to grave. These assessments should include metrics such as carbon footprint, water usage, and energy consumption to provide a holistic view of sustainability. End-of-life strategies, such as biodegradation, composting, or recycling, must be developed to enhance circular economy practices. For instance, biocomposites designed for disassembly can simplify recycling processes and reduce waste.

14.4.6 Application-specific research

Tailoring biocomposites for specific applications will maximize their utility and adoption. For example, lightweight biocomposites with high strength-to-weight ratios are ideal for automotive panels and aerospace components. In construction, biocomposites can replace conventional materials in nonstructural elements such as cladding and insulation. Long-term durability tests under various environmental conditions, including temperature extremes, UV exposure, and moisture, are necessary to validate performance and inform design improvements for targeted applications.

14.5 Recommendations for future research

Based on the findings, future research should focus on optimizing the Si/Al ratio to enhance both ultrahigh-strength and lightweight geopolymer concrete, exploring a broader range of materials like FA. Additionally, assessing long-term durability under various environmental conditions, such as chemical resistance and freeze-thaw cycles, is critical. A comprehensive analysis of the economic and environmental impacts, including life cycle costs, should also be conducted, particularly regarding the use of waste materials. Finally, application-specific testing, especially for precast elements and pavements, will help balance strength, weight, and performance for construction.

Biocomposite materials hold immense promise for a sustainable future, offering a pathway to reduce reliance on nonrenewable resources and mitigate environmental impact. However, addressing challenges related to raw material consistency, mechanical performance, cost, and scalability is essential to their broader adoption. By drawing lessons from parallel fields like geopolymer concrete and advancing research in material science, processing technologies, and economic modeling, biocomposites can become a cornerstone of sustainable development.

References

Abbas, W., Khalil, W., & Nasser, I. (2018). Production of lightweight geopolymer concrete using artificial local lightweight aggregate. *MATEC Web of Conferences, 162*. https://doi.org/10.1051/matecconf/201816202024, http://www.matec-conferences.org/.

Abdullah, M. M. A. B., Tahir, M. F. M., Tajudin, M. A. F. M. A., Ekaputri, J. J., Bayuaji, R., & Khatim, N. A. M. (2017). Study on the geopolymer concrete properties reinforced with hooked steel fiber. *IOP Conference Series: Materials Science and Engineering, 267*(1), 012014. https://doi.org/10.1088/1757-899x/267/1/012014.

Adamu, M., Rahman, M. R., & Hamdan, S. (2019). Formulation optimization and characterization of bamboo/polyvinyl alcohol/clay nanocomposite by response surface methodology. *Composites Part B: Engineering, 176*, 107297. https://doi.org/10.1016/j.compositesb.2019.107297.

Ahmad, J., Kontoleon, K. J., Majdi, A., Naqash, M. T., Deifalla, A. F., Ben Kahla, N., Isleem, H. F., & Qaidi, S. M. A. (2022). A comprehensive review on the ground granulated blast furnace slag (GGBS) in concrete production. *Sustainability (Switzerland), 14*(14). https://doi.org/10.3390/su14148783, http://www.mdpi.com/journal/sustainability/.

Ahmad, J., Pu, Z., Khan, K. A., Ahmad, I., Shaukat, A. J., Hao, Z., & Khan, I. (2022). A review on the effect of silica to alumina ratio, alkaline solution to binder ratio, calcium oxide + ferric oxide, molar concentration of sodium hydroxide and sodium silicate to sodium hydroxide ratio on the compressive strength of geopolymer concrete. *Silicon, 14*(7), 3147–3162. https://doi.org/10.1007/s12633-021-01130-3.

Ahmad Sofri, L., Mustafa Al Bakri Abdullah, M., Rosli Mohd Hasan, M., & Huang, Y. (2020). The influence of sodium hydroxide concentration on physical properties and strength development of high calcium fly ash based geopolymer as pavement base materials. *IOP Conference Series: Materials Science and Engineering*, *864*, 1, https://doi.org/10.1088/1757-899X/864/1/012016. https://iopscience.iop.org/journal/1757-899X.

Ahmed, H. U., Mohammed, A. A., & Mohammed, A. (2022). Soft computing models to predict the compressive strength of GGBS/FAgeopolymer concrete. *PLoS One, 17*(5). https://doi.org/10.1371/journal.pone.0265846, https://journals.plos.org/plosone/article/file?id=10.1371/journal.pone.0265846&type=printable.

Alamia, A., Gauducheau, V., Paisios, D., & VanRullen, R. (2020). Comparing feedforward and recurrent neural network architectures with human behavior in artificial grammar learning. *Scientific Reports, 10*(1). https://doi.org/10.1038/s41598-020-79127-y, www.nature.com/srep/index.html.

Alaneme, G. U., Olonade, K. A., Esenogho, E., & Lawan, M. M. (2024). Proposed simplified methodological approach for designing geopolymer concrete mixtures. *Nature Research, Uganda Scientific Reports, 14*(1). https://doi.org/10.1038/s41598-024-66093-y, https://www.nature.com/srep/.

Alashker, Y., & Raza, A. (2022). Seismic performance of recycled aggregate geopolymer concrete-filled double skin tubular columns with internal steel and external FRP tube. *Polymers, 14*(23). https://doi.org/10.3390/polym14235204, http://www.mdpi.com/journal/polymers.

Almutairi, A. L., Tayeh, B. A., Adesina, A., Isleem, H. F., & Zeyad, A. M. (2021). Potential applications of geopolymer concrete in construction: A review. *Case Studies in Construction Materials, 15*. https://doi.org/10.1016/j.cscm.2021.e00733, http://www.journals.elsevier.com/case-studies-in-construction-materials/.

Althoey, F., Zaid, O., Alsulamy, S., Martínez-García, R., de Prado-Gil, J., & Arbili, M. M. (2023). Experimental study on the properties of ultrahigh-strength geopolymer concrete with polypropylene fibers and nano-silica. *PLoS One, 18*(4). https://doi.org/10.1371/journal.pone.0282435, https://journals.plos.org/plosone/article/file?id=10.1371/journal.pone.0282435&type=printable.

Amran, M., Al-Fakih, A., Chu, S. H., Fediuk, R., Haruna, S., Azevedo, A., & Vatin, N. (2021). Long-term durability properties of geopolymer concrete: An in-depth review. *Case*

Studies in Construction Materials, 15, e00661. https://doi.org/10.1016/j.cscm.2021.e00661.

Artika H, N., MZ, Y., & MT, N. F. (2019). An overview of scheduled wastes management in malaysia. *Journal of Wastes and Biomass Management, 1*(2), 01–04. https://doi.org/10.26480/jwbm.02.2019.01.04.

Bakhoum, E. S., & Mater, Y. M. (2022). Decision analysis for the influence of incorporating waste materials on green concrete properties. *International Journal of Concrete Structures and Materials, 16*(1). https://doi.org/10.1186/s40069-022-00553-5, https://www.springer.com/journal/40069.

Bakri, M. K. B., Jayamani, E., Hamdan, S., Rahman, M. R., & Kakar, A. (2018). Potential of Borneo Acacia wood in fully biodegradable bio-composites' commercial production and application. *Polymer Bulletin, 75*(11), 5333–5354. https://doi.org/10.1007/s00289-018-2299-9, https://rd.springer.com/journal/289.

Bhaidas, J. N., Bhausaheb, M. D., Vijay, C. T., Bhanudas, G. S., Dnyaneshwar, D. H., Bhadane, P. J. P., & Borase, P. N. R. (2024). Advancements in lightweight concrete: A comprehensive review. *International Journal for Research in Applied Science and Engineering Technology, 12*(6), 1–2. https://doi.org/10.22214/ijraset.2024.62321.

Cao, R., Fang, Z., Jin, M., & Shang, Y. (2022). Application of machine learning approaches to predict the strength property of geopolymer concrete. *Materials, 15*(7). https://doi.org/10.3390/ma15072400, https://www.mdpi.com/1996-1944/15/7/2400/pdf.

Castillo, H., Collado, H., Droguett, T., Sánchez, S., Vesely, M., Garrido, P., & Palma, S. (2021). Factors affecting the compressive strength of geopolymers: A review. *Minerals, 11*(12). https://doi.org/10.3390/min11121317, https://www.mdpi.com/2075-163X/11/12/1317/pdf.

Chen, T., & Guestrin, C. (2016). XGBoost: A scalable tree boosting system. In *Proceedings of the ACM SIGKDD International Conference on Knowledge Discovery and Data Mining* 13-17 (pp. 785–794). https://doi.org/10.1145/2939672.2939785.

Chen, Y., de Lima, L. M., Li, Z., Ma, B., Lothenbach, B., Yin, S., Yu, Q., & Ye, G. (2024). Synthesis, solubility and thermodynamic properties of N-A-S-H gels with various target Si/Al ratios. *Cement and Concrete Research, 180*, 107484. https://doi.org/10.1016/j.cemconres.2024.107484.

Chiranjeevi, K., Abraham, M., Rath, B., & Praveenkumar, T. R. (2023). Enhancing the properties of geopolymer concrete using nano-silica and microstructure assessment: A sustainable approach. *Scientific Reports, 13*(1). https://doi.org/10.1038/s41598-023-44491-y, https://www.nature.com/srep/.

Chuah, S., Duan, W. H., Pan, Z., Hunter, E., Korayem, A. H., Zhao, X. L., Collins, F., & Sanjayan, J. G. (2016). The properties of fly ash based geopolymer mortars made with dune sand. *Materials and Design, 92*, 571–578. https://doi.org/10.1016/j.matdes.2015.12.070.

Chuewangkam, N., Kidkhunthod, P., & Pinitsoontorn, S. (2024). Direct evidence for the mechanism of early-stage geopolymerization process. *Case Studies in Construction Materials, 21*, e03539. https://doi.org/10.1016/j.cscm.2024.e03539.

Cong, P., & Cheng, Y. (2021). Advances in geopolymer materials: A comprehensive review. *Journal of Traffic and Transportation Engineering (English Edition, 8*(3), 283–314. https://doi.org/10.1016/j.jtte.2021.03.004, http://www.journals.elsevier.com/journal-of-traffic-and-transportation-engineering-english-edition.

Cui, Y., Ai, W., Tekle, B. H., Liu, M., Qu, S., & Zhang, P. (2023). State of the art review on the production and bond behaviour of reinforced geopolymer concrete. *Low-Carbon Materials and Green Construction, 1*(1). https://doi.org/10.1007/s44242-023-00027-1.

Dang, T. K. M., Nikzad, M., Arablouei, R., Masood, S., Bui, D.-K., Truong, V. K., & Sbarski, I. (2024). Experimental study and predictive modelling of damping ratio in hybrid polymer concrete. *Construction and Building Materials, 411*, 134541. https://doi.org/10.1016/j.conbuildmat.2023.134541.

Delgado-Plana, P., Rodríguez-Expósito, A., Bueno-Rodríguez, S., Pérez-Villarejo, L., Tobaldi, D. M., Labrincha, J. A., & Eliche-Quesada, D. (2021). Effect of activating solution modulus on the synthesis of sustainable geopolymer binders using spent oil bleaching earths as precursor. *Sustainability, 13*(13), 7501. https://doi.org/10.3390/su13137501.

Dinh, H. L., Liu, J., Doh, J.-H., & Ong, D. E. L. (2024). Influence of Si/Al molar ratio and ca content on the performance of fly ash-based geopolymer incorporating waste glass and GGBFS. *Construction and Building Materials, 411*, 134741. https://doi.org/10.1016/j.conbuildmat.2023.134741.

Fatema, K., Sharmin, A. A., Sharna, J. F., Haque, M. A., Rahman, M., Sarker, S., Kazi, M., Rahman, M. R., Namakka, M., Uzzaman, M., & Patwary, M. A. M. (2024). Antioxidant and antidiabetic effects of flemingia macrophylla leaf extract and fractions: In vitro, molecular docking, dynamic simulation, pharmacokinetics, and biological activity studies. *BioResources, 19*(3), 4960–4983. https://doi.org/10.15376/biores.19.3.4960-4983, https://bioresources.cnr.ncsu.edu/wp-content/uploads/2024/06/BioRes_19_3_4960_Fatema_SSHRSKRNUP_Antioxid_Antidiabet_Leaf_Extract_Docking_23487.pdf.

Gao, B., Li, Y., Jang, S., Son, H., Lee, H., & Bae, C. J. (2024). Effect of geopolymerization reaction on the flexural strength of kaolin-based systems. *Materials, 17*(10). https://doi.org/10.3390/ma17102223, http://www.mdpi.com/journal/materials.

Ghita, R., Logofatu, C., Negrila, C.-C., Ungureanu, F., Cotirlan, C., Manea, A.-S., Lazarescu, M.-F., & Ghic, C. (2011). *Study of SiO_2/Si interface by surface techniques*. InTech. https://doi.org/10.5772/23174.

Gomes, K. C., Carvalho, M., Diniz, D. D. P., Abrantes, R. D. C. C., Branco, M. A., & de Carvalho, P. R. O. (2019). Carbon emissions associated with two types of foundations: CP-II Portland cement-based composite vs. geopolymer concrete. *Revista Materia, 24*(4). https://doi.org/10.1590/s1517-707620190004.0850, http://www.scielo.br/pdf/rmat/v24n4/1517-7076-rmat-24-04-e12525.pdf.

Hajiabadi, S. H., Khalifeh, M., van Noort, R., & Silva Santos Moreira, P. H. (2023). Review on geopolymers as wellbore sealants: State of the art optimization for CO_2 exposure and perspectives. *ACS Omega, 8*(26), 23320–23345. https://doi.org/10.1021/acsomega.3c01777, pubs.acs.org/journal/acsodf.

Hanani Ismail, A., Kusbiantoro, A., Tajunnisa, Y., Jaya Ekaputri, J., & Laory, I. (2024). A review of aluminosilicate sources from inorganic waste for geopolymer production: Sustainable approach for hydrocarbon waste disposal. *Cleaner Materials, 13*, 100259. https://doi.org/10.1016/j.clema.2024.100259.

Hari, H. P., Jayamani, E., Soon, K. H., Wong, Y. C., Rahman, M. R., & Bakri, M. K. B. (2021). Interfacial polarization effects on dielectric properties in flax reinforced polypropylene/strontium titanate composites. *Materials Chemistry and Physics, 265*. https://doi.org/10.1016/j.matchemphys.2021.124489, http://www.journals.elsevier.com/materials-chemistry-and-physics.

Haruna, S., Mohammed, B. S., & Wahab, M. M. A. (2020). Effect of GGBS slag on setting time and compressive strength of one-part geopolymer binders. *Journal of Infrastructure & Facility Asset Management, 2*(2). https://doi.org/10.12962/jifam.v2i2.7640.

Hong, X., Lee, J. C., & Qian, B. (2022). Mechanical properties and microstructure of high-strength lightweight concrete incorporating graphene oxide. *Nanomaterials, 12*(5), 833. https://doi.org/10.3390/nano12050833.

Huynh, A. T., Nguyen, Q. D., Xuan, Q. L., Magee, B., Chung, T., Tran, K. T., & Nguyen, K. T. (2020). A machine learning-assisted numerical predictor for compressive strength of geopolymer concrete based on experimental data and sensitivity analysis. *Applied Sciences (Switzerland), 10*(21), 1–16. https://doi.org/10.3390/app10217726, https://www.mdpi.com/2076-3417/10/21/7726/pdf.

Iffat, S. (2016). The characteristics of brick aggregate concrete on a basis of dry density and durability. *Malaysian Journal of Civil Engineering, 28*, 50–58.

Institutes, G. (n.d.). *Geopolymer cement for mitigation of global warming*. Geopolymer Institute.

Iqbal, M., Ashraf, M., Nazar, S., Alkhattabi, L., Alam, J., Alabduljabbar, H., & Khan, Z. (2024). Development of innovative alkali activated paste reinforced with polyethylene fibers for concrete crack repair. *PLoS One, 19*(7). https://doi.org/10.1371/journal.pone.0305143, https://journals.plos.org//plosone/article?id=10.1371/journal.pone.0305143.

Jain, L. C., Behera, H. S., Mandal, J. K., & Mohapatra, D. P. (2015). Computational intelligence in data mining – Volume 2: Proceedings of the international conference on CIDM, 20-21 December 2014. In *Smart innovation, systems and technologies* (vol. 32). https://doi.org/10.1007/978-81-322-2208-8. http://www.springer.com/series/8767.

James, A., Rezaur Rahman, M., Anwar Mohamed Said, K., Namakka, M., Kuok Kuok, K., Uddin Khandaker, M., Al-Humaidi, J. Y., Althomali, R. H., & Rahman, M. M. (2024). Lithium chloride-mediated enhancement of dye removal capacity in *Borneo bamboo* derived nanocellulose-based nanocomposite membranes (NCMs). *Journal of Molecular Liquids, 413*, 125973. https://doi.org/10.1016/j.molliq.2024.125973.

Jayamani, E., Hamdan, S., Kok Heng, S., Rahman, M. R., & Bin Bakri, M. K. (2016). Acoustical, thermal, and morphological properties of zein reinforced oil palm empty fruit bunch fiber bio-composites. *Journal of Applied Polymer Science, 133*(43). https://doi.org/10.1002/app.44164, http://onlinelibrary.wiley.com/journal/10.1002/(ISSN)1097-4628.

Jayamani, E., Hamdan, S., Rahman, M. R., Bakri, M. K. B., & Kakar, A. (2015). An investigation of sound absorption coefficient on sisal fiber poly lactic acid bio-composites. *Journal of Applied Polymer Science, 132*(34). https://doi.org/10.1002/app.42470, http://onlinelibrary.wiley.com/journal/10.1002/(ISSN)1097-4628.

Jayamaui, E., Rahman, M. R., Benhur, D. A., Bakri, M. K. B., Kakair, A., & Khan, A. (2020). Comparative study of fly ash/sugarcane fiber reinforced polymer composites properties. *BioResources, 15*(3), 5514–5531. https://doi.org/10.15376/biores.15.3.5514-5531, https://bioresources.cnr.ncsu.edu/wp-content/uploads/2020/05/BioRes_15_3_5514_Jayamani_RBBK_Comparative-Study_FLy-Ash_Sugarcane-Fiber_Reinforced_Polymer_17489.pdf.

Joshi, A., & Tiwari, H. (2023). An overview of python libraries for data science. *Journal of Engineering Technology and Applied Physics, 5*(2), 85–90. https://doi.org/10.33093/jetap.2023.5.2.10.

Kalinowska-Wichrowska, K., Pawluczuk, E., Bołtryk, M., & Nietupski, A. (2022). Geopolymer concrete with lightweight artificial aggregates. *Materials, 15*(9). https://doi.org/10.3390/ma15093012, https://www.mdpi.com/1996-1944/15/9/3012/pdf.

Kanagaraj, B., Anand, N., Praveen, B., Kandasami, S., Lubloy, E., & Naser, M. Z. (2023). Physical characteristics and mechanical properties of a sustainable lightweight geopolymer based self-compacting concrete with expanded clay aggregates. *Developments in the Built Environment, 13*, 100115. https://doi.org/10.1016/j.dibe.2022.100115.

Kanagaraj, B., Lubloy, E., Anand, N., Hlavicka, V., & Kiran, T. (2023). Investigation of physical, chemical, mechanical, and microstructural properties of cement-less concrete – State-of-the-art review. *Construction and Building Materials, 365*, 130020. https://doi.org/10.1016/j.conbuildmat.2022.130020.

Kathirvel, P., & Sreekumaran, S. (2021). Sustainable development of ultra high performance concrete using geopolymer technology. *Journal of Building Engineering, 39*. https://doi.org/10.1016/j.jobe.2021.102267, http://www.journals.elsevier.com/journal-of-building-engineering/.

Kiew, K. S., Hamdan, S., & Rahman, M. R. (2013). Comparative study of dielectric properties of chicken feather/kenaf fiber reinforced unsaturated polyester composites. *North Carolina State University, Malaysia BioResources, 8*(2), 1591–1603. https://doi.org/10.15376/biores.8.2.1591-1603, http://www.ncsu.edu/bioresources/BioRes_08/BioRes_08_2_1591_Kiew_HR_Dielectric_Prop_Feather_Kenaf_PE_Composite_3628.pdf.

Kucukgoncu, H., & Özbayrak, A. (2024). Microstructural analysis of low-calcium fly ash-based geopolymer concrete with different ratios of activator and binder under high temperatures. *Arabian Journal for Science and Engineering*. https://doi.org/10.1007/s13369-024-09266-1, https://www.springer.com/journal/13369.

Kuok, K. K., Bakri, M. K. B., Chan, C. P., Rahman, M. R., Namakka, M., Said, K. A. M., Yun, C. M., & Rahman, M. M. (2024). Merits of bamboo utilization in earth preservation, water and wastewater treatment: A mini review. *BioResources, 19*(2), 1–24. https://doi.org/10.15376/biores.19.2.Kuok, https://bioresources.cnr.ncsu.edu/wp-content/uploads/2024/03/BioRes_19_2_Review_Kuok_BCRNSYR_Merits_Bamboo_Utiliz_Water_Treatment_23312.pdf.

Kushwah, S., Mudgal, M., & Chouhan, R. K. (2021). The process, characterization and mechanical properties of fly ash-based Solid form geopolymer via mechanical activation. *South African Journal of Chemical Engineering, 38*, 104–114. https://doi.org/10.1016/j.sajce.2021.09.002, https://www.journals.elsevier.com/south-african-journal-of-chemical-engineering/.

Lai, J. C. H., Rahman, M. R., Hamdan, S., Liew, F. K., Rahman, M. M., & Hossen, M. F. (2015). Impact of nanoclay on physicomechanical and thermal analysis of polyvinyl alcohol/fumed silica/clay nanocomposites. *Journal of Applied Polymer Science, 132*(15). https://doi.org/10.1002/app.41843, http://onlinelibrary.wiley.com/journal/10.1002/(ISSN)1097-4628.

Lao, J. C., Xu, L. Y., Huang, B. T., Dai, J. G., & Shah, S. P. (2022). Strain-hardening ultra-high-performance geopolymer concrete (UHPGC): Matrix design and effect of steel fibers. *Composites Communications, 30*. https://doi.org/10.1016/j.coco.2022.101081, http://www.journals.elsevier.com/composites-communications.

Lao, J. C., Xu, L. Y., Huang, B. T., Zhu, J. X., Khan, M., & Dai, J. G. (2023). Utilization of sodium carbonate activator in strain-hardening ultra-high-performance geopolymer concrete (SH-UHPGC). *Frontiers in Materials, 10*. https://doi.org/10.3389/fmats.2023.1142237, journal.frontiersin.org/journal/materials.

Lăzărescu, A. V., Szilagyi, H., Baeră, C., & Ioani, A. (2017). The effect of alkaline activator ratio on the compressive strength of fly ash-based geopolymer paste. *IOP Conference Series: Materials Science and Engineering*, *209*, 1. https://doi.org/10.1088/1757-899X/209/1/012064. http://www.iop.org/EJ/journal/mse.

Li, Z., Zhang, J., & Wang, M. (2020). Structure, reactivity, and mechanical properties of sustainable geopolymer material: A reactive molecular dynamics study. *Frontiers in Materials, 7*. https://doi.org/10.3389/fmats.2020.00069, journal.frontiersin.org/journal/materials.

Liu, Y., Zhang, Z., Shi, C., Zhu, D., Li, N., & Deng, Y. (2020). Development of ultra-high performance geopolymer concrete (UHPGC): Influence of steel fiber on mechanical properties. *Cement and Concrete Composites, 112*. https://doi.org/10.1016/j.cemconcomp.2020.103670, http://www.sciencedirect.com/science/journal/09589465.

Ma, R. Y., Yang, J., & Peng, G. F. (2023). Influence of steel fiber types on residual mechanical properties and explosive spalling of hybrid fiber reinforced ultra-high performance concrete: Optimization and evaluations. *Case Studies in Construction Materials, 19*. https://doi.org/10.1016/j.cscm.2023.e02538, http://www.journals.elsevier.com/case-studies-in-construction-materials/.

Madadi, A., & Wei, J. (2022). Characterization of calcium silicate hydrate gels with different calcium to silica ratios and polymer modifications. *Gels, 8*(2). https://doi.org/10.3390/gels8020075, https://www.mdpi.com/2310-2861/8/2/75/pdf.

Madirisha, M. M., Dada, O. R., & Ikotun, B. D. (2024). Chemical fundamentals of geopolymers in sustainable construction. *Materials Today Sustainability, 27*. https://doi.org/10.1016/j.mtsust.2024.100842, https://www.sciencedirect.com/science/journal/25892347.

Marini, L., Mannan, M. A., Kueh, A. B. H., Abdullah, A. A., Abed, F., & Gunasekaran, K. (2024). An analysis of the environmental effects of three types of concrete: Ready-mixed, reactive powder, and geopolymer. *Ain Shams Engineering Journal, 15*(9), 102926. https://doi.org/10.1016/j.asej.2024.102926.

Memon, F. A., Nuruddin, M. F., Demie, S., & Shafiq, N. (2012). Effect of superplasticizer and extra water on workability and compressive strength of self-compacting geopolymer concrete. *Research Journal of Applied Sciences, Engineering and Technology, 4*(5), 407–414. http://maxwellsci.com/print/rjaset/v4-407-414.pdf Malaysia.

Murali, G., Nassar, A. K., Swaminathan, M., Kathirvel, P., & Wong, L. S. (2024). Effect of silica fume and glass powder for enhanced impact resistance in GGBFS-based ultra high-performance geopolymer fibrous concrete: An experimental and statistical analysis. *Defence Technology, 41*, 59–81. https://doi.org/10.1016/j.dt.2024.05.015, https://www.sciencedirect.com/science/journal/22149147.

Mustofa, M., & Pintowantoro, S. (2016). The effect of Si/Al ratio to compressive strength and water absorption of ferronickel. *International Seminar on Science and Technology*, (2016), 167–172.

Namakka, M., Rahman, M. R., Bin Mohamad Said, K. A., & Muhammad, A. (2024). Insights into micro-and nano-zero valent iron materials: Synthesis methods and multifaceted applications. *RSC Advances, 14*(41), 30411–30439. https://doi.org/10.1039/d4ra03507k, http://pubs.rsc.org/en/journals/journal/ra.

Namakka, M., Rahman, M. R., Mohamad Bin Said, K. A., Kuok, K. K., Md Yusof, F. A., Al-Saleem, M. S. M., Al-Humaidi, J. Y., & Rahman, M. M. (2024). Unveiling the synergistic effect of an nZVI-SiO_2-TiO_2 nanocomposite for the remediation of dye contaminated wastewater. *Materials Advances, 5*(23), 9292–9313. https://doi.org/10.1039/d4ma00853g, https://www.rsc.org/journals-books-databases/about-journals/materials-advances/.

Namakka, M., Rahman, M. R., Said, K. A. M. B., Abdul Mannan, M., & Patwary, A. M. (2023). A review of nanoparticle synthesis methods, classifications, applications, and characterization. *Environmental Nanotechnology, Monitoring and Management, 20*. https://doi.org/10.1016/j.enmm.2023.100900, http://www.journals.elsevier.com/environmental-nanotechnology-monitoring-and-management/.

Ndagi, A., & Saleh Jaafar, M. (2019). Geo-polymer binder as portland cement alternative: Challenges, current developments and future prospects. *Jurnal Kejuruteraan, 31*(2), 281–286. https://doi.org/10.17576/jkukm-2019-31(2)-12.

Neupane, K. (2022). Evaluation of environmental sustainability of one-part geopolymer binder concrete. *Cleaner Materials, 6*, 100138. https://doi.org/10.1016/j.clema.2022.100138.

Nukah, P. D., Abbey, S. J., Booth, C. A., & Oti, J. (2024). Development of low carbon concrete and prospective of geopolymer concrete using lightweight coarse aggregate and cement

replacement materials. *Construction and Building Materials, 428*. https://doi.org/10.1016/j.conbuildmat.2024.136295, https://www.sciencedirect.com/science/journal/09500618.

Pacheco-Torgal, F., Jalali, S., Labrincha, J., & John, V. M. (2013). *Eco-efficient concrete eco-efficient concrete*. Elsevier, 1–595. https://www.sciencedirect.com/book/9780857094247.

Palomo, A., Grutzeck, M. W., & Blanco, M. T. (1999). Alkali-activated fly ashes: A cement for the future. *Cement and Concrete Research, 29*(8), 1323–1329. https://doi.org/10.1016/S0008-8846(98)00243-9.

Qaidi, S. M. A., Sulaiman Atrushi, D., Mohammed, A. S., Unis Ahmed, H., Faraj, R. H., Emad, W., Tayeh, B. A., & Mohammed Najm, H. (2022). Ultra-high-performance geopolymer concrete: A review. *Construction and Building Materials, 346*. https://doi.org/10.1016/j.conbuildmat.2022.128495, https://www.journals.elsevier.com/construction-and-building-materials.

Qaidi, S., Najm, H. M., Abed, S. M., Ahmed, H. U., Al Dughaishi, H., Al Lawati, J., Sabri, M. M., Alkhatib, F., & Milad, A. (2022). Fly ash-based geopolymer composites: A review of the compressive strength and microstructure analysis. *Materials, 15*(20), 7098. https://doi.org/10.3390/ma15207098.

Qamar, R., & Ali Zardari, B. (2023). Artificial neural networks: An overview. *Mesopotamian Journal of Computer Science,* 130–139. https://doi.org/10.58496/mjcsc/2023/015.

Rahardjo, A., Navaratnam, S., Zhang, G., Tushar, Q., & Nguyen, K. (2024). Suitability of foamed concrete for the composite floor system in mid-to-high-rise modular buildings: Design, structural, and sustainability perspectives. *Sustainability (Switzerland), 16*(4). https://doi.org/10.3390/su16041624, http://www.mdpi.com/journal/sustainability/.

Rahman, M. R., Hamdan, S., Ahmed, A. S., Islam, M. S., Talib, Z. A., Abdullah, W. F. W., & Mat, M. S. C. (2011). Thermogravimetric analysis and dynamic Young's modulus measurement of *N*,*N*-dimethylacetamide-impregnated wood polymer composites. *Journal of Vinyl and Additive Technology, 17*(3), 177–183. https://doi.org/10.1002/vnl.20275.

Rahman, M. R., Hamdan, S., Hasan, M., Baini, R., & Salleh, A. A. (2015). Physical, mechanical, and thermal properties of wood flour reinforced maleic anhydride grafted unsaturated polyester (UP) biocomposites. *BioResources, 10*(3), 4557–4568. https://doi.org/10.15376/biores.10.3.4557-4568, https://www.ncsu.edu/bioresources/BioRes_10/BioRes_10_3_4557_Rahman_HHBS_Phys_Mech_Therm_Prop_Wood_Flour_Reinf_7280.pdf.

Rahman, M. R., Hamdan, S., Hashim, D. M. A., Islam, M. S., & Takagi, H. (2015). Bamboo fiber polypropylene composites: Effect of fiber treatment and nano clay on mechanical and thermal properties. *Journal of Vinyl and Additive Technology, 21*(4), 253–258. https://doi.org/10.1002/vnl.21407, http://onlinelibrary.wiley.com/journal/10.1002/(ISSN)1548-0585.

Rahman, M. R., Hamdan, S., Jayamani, E., Kakar, A., Bakri, M. K. B., & Yusof, F. A. B. M. (2019). Tert-butyl catechol/alkaline-treated kenaf/jute polyethylene hybrid composites: Impact on physico-mechanical, thermal and morphological properties. *Polymer Bulletin, 76*(2), 763–784. https://doi.org/10.1007/s00289-018-2404-0.

Rahman, M. R., Hamdan, S., Lai, J. C. H., Jawaid, M., & Yusof, F. A. B. M. (2017). Physico-mechanical, thermal and morphological properties of furfuryl alcohol/2-ethylhexyl methacrylate/halloysite nanoclay wood polymer nanocomposites (WPNCs). *Heliyon, 3*(7). https://doi.org/10.1016/j.heliyon.2017.e00342, http://www.journals.elsevier.com/heliyon/.

Rahman, M. R., Hui, J. L. C., Hamdan, S., Ahmed, A. S., Baini, R., & Saleh, S. F. (2013). Combined styrene/MMA/nanoclay cross-linker effect on wood-polymer composites (WPCs). *BioResources, 8*(2), 4227–4237. http://www.ncsu.edu/bioresources/Back_Issues.htm.

Rahman, M. R., James, A., Mohamed Said, K. A., Namakka, M., Khandaker, M. U., Jiunn, W. H., Al-Humaidi, J. Y., Althomali, R. H., & Rahman, M. M. (2024). A TiO_2 grafted bamboo derivative nanocellulose polyvinylidene fluoride (PVDF) nanocomposite membrane for wastewater treatment by a photocatalytic process. *Materials Advances, 5*(19), 7617–7636. https://doi.org/10.1039/d4ma00716f, https://www.rsc.org/journals-books-databases/about-journals/materials-advances/.

Rajalekshmi, P., & Jose, P. A. (2023). Influence of eco-friendly lightweight aggregates in mechanical and durability properties of geopolymer concrete. *Revista Materia, 28*(4). https://doi.org/10.1590/1517-7076-RMAT-2023-0209, https://www.scielo.br/j/rmat/a/zWKmLYWmMJnbVSsPKS7ytMt/?lang=en&format=pdf.

Rathnayaka, M., Karunasinghe, D., Gunasekara, C., Wijesundara, K., Lokuge, W., & Law, D. W. (2024). Machine learning approaches to predict compressive strength of fly ash-based geopolymer concrete: A comprehensive review. *Construction and Building Materials, 419*. https://doi.org/10.1016/j.conbuildmat.2024.135519, https://www.sciencedirect.com/science/journal/09500618.

Rintala, A., Havukainen, J., & Abdulkareem, M. (2021). Estimating the cost-competitiveness of recycling-based geopolymer concretes. *Recycling, 6*(3). https://doi.org/10.3390/recycling6030046, https://www.mdpi.com/2313-4321/6/3/46/pdf.

Rodacka, M., Domagała, L., & Szydłowski, R. (2023). Assessment of properties of structural lightweight concrete with sintered fly ash aggregate in terms of its suitability for use in prestressed members. *Materials, 16*(15). https://doi.org/10.3390/ma16155429, http://www.mdpi.com/journal/materials.

Rumsys, D., Spudulis, E., Bacinskas, D., & Kaklauskas, G. (2018). Compressive strength and durability properties of structural lightweight concrete with fine expanded glass and/or clay aggregates. *Materials, 11*(12). https://doi.org/10.3390/ma11122434, https://www.mdpi.com/1996-1944/11/12/2434/pdf.

Sax, S., (2024). How the cement industry is creating carbon-negative building materials.

Schneider, A., Hommel, G., & Blettner, M. (2010). Lineare regressionsanalyse – Teil 14 der serie zur bewertung wissenschaftlicher publikationen. *Deutsches Arzteblatt, 107*(44), 776–782. https://doi.org/10.3238/arztebl.2010.0776Germany, http://www.aerzteblatt.de/v4/archiv/pdf.asp?id=78996.

Siddika, A., Hajimohammadi, A., Ferdous, W., & Sahajwalla, V. (2021). Roles of waste glass and the effect of process parameters on the properties of sustainable cement and geopolymer concrete—A state-of-the-art review. *Polymers, 13*(22). https://doi.org/10.3390/polym13223935, https://www.mdpi.com/2073-4360/13/22/3935/pdf.

Singh, K. K., & Kumar, M. U. (2024). The empirical investigation of lightweight concrete via the utilization of varied waste materials, *International Research Journal of Engineering and Technology (IRJET)*, *11*(5), 1435–1440..

Sueraya, A. Z., Rahman, M. R., Said, K. A. B. M., Namakka, M., Kanakaraju, D., Al-Humaidi, J. Y., Al-Baqami, S. M., Rahman, M. M., & Khandaker, M. U. (2024). Impact of titanium dioxide/graphene in polyvinylidene fluoride nanocomposite membrane to intensify methylene blue dye removal, antifouling performance, and reusability. *Journal of Applied Polymer Science, 141*(47). https://doi.org/10.1002/app.56257, http://onlinelibrary.wiley.com/journal/10.1002/(ISSN)1097-4628.

Tahwia, A. M., Heniegal, A. M., Abdellatief, M., Tayeh, B. A., & Elrahman, M. A. (2022). Properties of ultra-high performance geopolymer concrete incorporating recycled waste glass. *Case Studies in Construction Materials, 17*. https://doi.org/10.1016/j.cscm.2022.e01393, http://www.journals.elsevier.com/case-studies-in-construction-materials/.

Tempest, B., Snell, C., Gentry, T., Trejo, M., & Isherwood, K. (2015). Manufacture of full-scale geopolymer cement concrete components: A case study to highlight opportunities and challenges. *PCI Journal, 60*(6), 39–50. https://doi.org/10.15554/pcij.11012015.39.50, http://www.pci.org/uploadedFiles/Siteroot/Publications/PCI_Journal/2015/November/Tempest_ND15_Web.pdf.

Tu, W., & Zhang, M. (2023). Behaviour of alkali-activated concrete at elevated temperatures: A critical review. *Cement and Concrete Composites, 138*, 104961. https://doi.org/10.1016/j.cemconcomp.2023.104961.

Usman Kankia, M., Baloo, L., Danlami, N., Zawawi, N. A., Bello, A., & Muhammad, S. I. (2023). Microstructural analysis and compressive strength of fly ash and petroleum sludge ash geopolymer mortar under high temperatures. *Sustainability (Switzerland), 15*(12). https://doi.org/10.3390/su15129846, http://www.mdpi.com/journal/sustainability/.

Van Dao, D., Ly, H. B., Trinh, S. H., Le, T. T., & Pham, B. T. (2019). Artificial intelligence approaches for prediction of compressive strength of geopolymer concrete. *Materials, 12*(6). https://doi.org/10.3390/ma12060983, https://res.mdpi.com/materials/materials-12-00983/article_deploy/materials-12-00983.pdf.

Vázquez-Calle, K., Guillén-Mena, V., & Quesada-Molina, F. (2022). Analysis of the embodied energy and CO_2 emissions of ready-mixed concrete: A case study in Cuenca, Ecuador. *Materials, 15*(14). https://doi.org/10.3390/ma15144896, http://www.mdpi.com/journal/materials.

Verma, N. K., Rao, M. C., & Kumar, S. (2022). Effect of curing regime on compressive strength of geopolymer concrete. *IOP Conference Series: Earth and Environmental Science*, *982*, 1. https://doi.org/10.1088/1755-1315/982/1/012031, https://iopscience.iop.org/journal/1755-1315.

Wang, L. J., Liu, Y. Q., Wang, Q., & Chou, K. C. (2015). Evolution mechanisms of $MgO{\cdot}Al_2O_3$ inclusions by cerium in spring steel used in fasteners of high-speed railway. *ISIJ International, 55*(5), 970–975. https://doi.org/10.2355/isijinternational.55.970, https://www.jstage.jst.go.jp/article/isijinternational/55/5/55_970/_pdf.

Wang, R., Zhang, J., Lu, Y., Ren, S., & Huang, J. (2024). Towards a reliable design of geopolymer concrete for green landscapes: A comparative study of tree-based and regression-based models. *Buildings, 14*(3), 615. https://doi.org/10.3390/buildings14030615.

Wei, X., Ming, F., Li, D., Chen, L., & Liu, Y. (2020). Influence of water content on mechanical strength and microstructure of alkali-activated fly ash/GGBFS mortars cured at cold and polar regions. *Materials, 13*(1). https://doi.org/10.3390/ma13010138, https://res.mdpi.com/d_attachment/materials/materials-13-00138/article_deploy/materials-13-00138.pdf.

Wong, L. S. (2022). Durability performance of geopolymer concrete: A review. *Polymers, 14*(5). https://doi.org/10.3390/polym14050868, https://www.mdpi.com/2073-4360/14/5/868/pdf.

Zaki, A., Putri, O., Yadi, S., & Rommel, E. (2021). Mechanical behavior of corroded steel in lightweight concrete: A review. *IOP Conference Series: Earth and Environmental Science*, *832*, 1. https://doi.org/10.1088/1755-1315/832/1/012015 https://iopscience.iop.org/journal/1755-1315.

Zheng, J., Qi, L., Zheng, Y., & Zheng, L. (2023). Mechanical properties and compressive constitutive model of steel fiber-reinforced geopolymer concrete. *Journal of Building Engineering, 80*. https://doi.org/10.1016/j.jobe.2023.108161, http://www.journals.elsevier.com/journal-of-building-engineering/.

Index

Note: Page numbers followed by "*f*" and "*t*" refer to figures and tables, respectively.

WOODHEAD PUBLISHING SERIES IN COMPOSITES SCIENCE AND ENGINEERING

Smart Biocomposite Materials: Fabrication, Applications, and Sustainability presents the latest advancements in this important research field. This book starts with a brief introduction to the classification of these materials and proceeds to discuss their innovative fabrication techniques. There is also a dedicated chapter on functional fillers. This book offers a holistic view, covering mechanical performance, environmental impact, bio-sustainability, high-performance applications, and their practical implementation. It also addresses ethical, cultural, and societal aspects as well as key challenges and future directions.

This book offers a comprehensive examination of the environmental aspects and provides in-depth technical insights into the science and engineering of these materials, helping professionals to make informed decisions about adopting these sustainable materials in their future research projects.

Key Features

- Presents the latest research findings on the properties, manufacturing, and potential future applications of intelligent biocomposite materials
- Includes practical guidelines and best practices for incorporating intelligent biocomposite materials into various industrial products, offering step-by-step approaches and real-world examples
- Provides quantifiable sustainability metrics and LCA, helping readers to assess the environmental impact of their material choices, to make informed decisions
- Covers applications in intelligent sensors and actuators, in drug delivery, and in biomedical, aerospace, automotive, and construction sectors
- Features case studies from various global regions and industries to showcase how these materials can be used in different cultural and economic contexts, emphasizing the inclusivity of sustainable practices

About the Editors

Md. Rezaur Rahman - Department of Chemical Engineering, Faculty of Engineering, University Malaysia Sarawak, Kota Samarahan, Sarawak, Malaysia.

Muhammad Khusairy Bin Bakri - Composite Materials and Engineering Center, Washington State University, Pullman, WA, United States.

ELSEVIER

WP
WOODHEAD PUBLISHING
An imprint of Elsevier
shop.elsevier.com

ISBN 978-0-443-33643-0
9 780443 336430